

https://dspace.org/

The effect of voltage dips on wound rotor induction motors used in slip energy recovery drives – implications for converters

Davies, Simon Quail

2006-10-31T10:14:50Z
http://hdl.handle.net/10539/1523

Downloaded from a DSpace repository. https://dspace.org/

The effect of voltage dips on wound rotor induction motors used in slip energy recovery drives – implications for converters

Simon Quail Davies

A dissertation submitted to the Faculty of Engineering and the Built Environment, University of the Witwatersrand, Johannesburg, in partial fulfilment of the requirements for the degree of Master of Science in Engineering

Johannesburg, October 2005

Declaration

I declare that this dissertation is my own, unaided work, except where otherwise acknowledged. It is being submitted in partial fulfilment of the degree of Master in Science in Engineering in the University of the Witwatersrand, Johannesburg. It has not been submitted before for any degree or examination in any other university.

Signed this ___ day of _____ 20___

_____

Simon Quail Davies

Abstract

Slip energy recovery (SER) drives are used extensively in industry as they offer cost effective speed control of large wound rotor induction motors. The biggest disadvantage associated with the use of SER drives is the vulnerability of the rotor circuit converters to power system disturbances such as voltage dips. The failure of converters as a result of voltage dips is a problem associated with the use of these particular drives.

The aim of this research is to better understand the stresses on rotor circuit converters as a result of voltage dips at the terminals of the motor. The rotor transients developed by a wound rotor induction motor are investigated for a range of three phase and single phase voltage dips. Simulations conducted in the Alternative Transients Program (ATP) supplement measurements conducted on a simplified SER circuit. The results confirm that voltage dips cause significant stresses on the converters in the rotor circuit. Good correlation was obtained between simulated and measured results. This work allows for a better understanding of the response of wound rotor induction motors to voltage dips and identifies the threat that voltage dips impose on the SER rotor circuit converters.

To my Mom, Dad and family, thank you for your love and support

Acknowledgements

Thanks to John Van Coller for his guidance with regard to the topic and the research. To Harry Fellows and all the guys in the GENMIN lab, thank you for all the assistance.

Contents

Declaration i
Abstract ii
Acknowledgements iv
Contents v
List of figures vii
List of tables viii
Appendix A 11
Simulation 11
A.1 Dynamic modelling of induction motors 11
A.2 d-q fundamentals 12
A.3 Slip energy recovery test circuit 15
A.3.1 Leakage inductance saturation 17
A.3.2 Controlled voltage source 17
A.3.3 Diode bridge model 17
A.3.4 Induction motor load model 18
A.3.5 Simulation comments 18
A.4 Simulation results 19
A.4.1 Three phase results 20
A.4.2 Single phase results 21
Appendix B 24
Measurements 24
B.1 Three phase dips 24
B.1.1. 0.2 p.u balanced three phase dips 25
B.1.2. 0.4 p.u balanced three phase dips 29
B.1.3. 0.6 p.u balanced three phase dips 33
B.1.4. Discussion of balanced three phase dip results 37
B.2 Single phase dips 38
B.2.1. Discussion of single phase dip results 42

B.3 Varied rotor resistance 43
References 47

List of figures

Figure A.1. Stator current space vector and stator phase currents 13
Figure A.2. Simulation test circuit 16
Figure A.3. 100 ms dip results (0.4 p.u. balanced three phase dip) 21
Figure A.4. 100 ms dip results (0.4 p.u. single phase dip) 23
Figure B.1. 10 ms dip results (0.2 p.u. balanced three phase dip) 26
Figure B.2. 20ms dip results (0.2 p.u. balanced three phase dip) 27
Figure B.3. 100 ms dip results (0.2 p.u. balanced three phase dip) 28
Figure B.4. 10 ms dip results (0.4 p.u. balanced three phase dip) 30
Figure B.5. 20ms dip results (0.4 p.u. balanced three phase dip) 31
Figure B.6. 100 ms dip results (0.4 p.u. balanced three phase dip) 32
Figure B.7. 10 ms dip results (0.6 p.u. balanced three phase dip) 34
Figure B.8. 20ms dip results (0.6 p.u. balanced three phase dip) 35
Figure B.9. 100 ms dip results (0.6 p.u. balanced three phase dip) 36
Figure B.10. 10 ms dip results (0.4 p.u. single phase dip – maximum flux linkage) . 39
Figure B.11. 10 ms dip results (0.4 p.u. single phase dip – minimum flux linkage) .. 40
Figure B.12. 100 ms dip results (0.4 p.u. single phase dip – maximum flux linkage) 41
Figure B.13. 10 ms dip results (0.6 p.u. three phase dip – 0.4 ohm rotor resistance). 44
Figure B.14. 50 ms dip results (0.6 p.u. three phase dip – 0.4 ohm rotor resistance). 45
Figure B.15. 100 ms dip results (0.6 p.u. three phase dip – 0.4 ohm rotor resistance) 46

List of tables

Table B.1: Measurement equipment 24
Table B.2: Balanced three phase 0.2 p.u. dip results 25
Table B.3: Balanced three phase 0.4 p.u. dip results 29
Table B.4: Balanced three phase 0.6 p.u. dip results 33
Table B.5: Single phase dip results 38
Table B.6: 0.4 ohm rotor resistance three phase dip results 43

THE EFFECT OF VOLTAGE DIPS ON WOUND ROTOR INDUCTION MOTORS USED IN SLIP ENERGY RECOVERY DRIVES – IMPLICATIONS FOR CONVERTERS

S. Q. Davies

School of Electrical & Information Engineering, University of the Witwatersrand, Johannesburg, South Africa

Abstract: Slip energy recovery (SER) drives are used extensively in industry as they offer cost effective speed control of large wound rotor induction motors. The biggest disadvantage associated with the use of SER drives is the vulnerability of the rotor circuit converters to power system disturbances such as voltage dips. The failure of converters as a result of voltage dips is a problem associated with the use of these drives. The aim of this research is to better understand the stresses on rotor circuit converters as a result of voltage dips at the terminals of the motor. The rotor transients developed by a wound rotor induction motor are investigated for a range of three phase and single phase voltage dips. Simulations conducted with the Alternative Transients Program (ATP) supplement measurements conducted on a simplified SER circuit. The results confirm that voltage dips cause significant stresses on the converters in the rotor circuit. The balance of mmf in the motor at the instant of the voltage dip and at the point of voltage recovery is the cause of large transient rotor currents which result in large over-voltages in the rotor circuit. The theorem of constant flux linkage and the effect of remnant (trapped) flux present in the motor are responsible for large transient rotor currents developed at voltage recovery which tend to be more significant for shorter duration dips. Good correlation was obtained between simulated and measured results and allow for a better understanding of the response of wound rotor induction motors to voltage dips. This is very important if SER converters are to be improved from a control perspective.

Key words: Slip energy recovery, trapped flux, voltage dips, wound rotor induction motors.

1. INTRODUCTION

SER drives provide a cost effective means of achieving speed control of large induction motors and have been used extensively in industry driving mill, fan and pump loads. These drives are advantageous as they offer a wide range of speed control at high efficiency [1]. The most significant problem associated with the use of SER drives is the vulnerability of the rotor converters to supply disturbances such as voltage dips. There have been many recorded failures of SER converters as a result of voltage dips at the supply terminals of the motors.

Specific control strategies and protection circuitry have been developed to ensure rotor circuit converters can ride through system disturbances such as voltage dips [2, 3]. However, the reduction of electrical transients by adopting these techniques can be ineffectual if a good understanding does not exist as to what is happening from the motor's perspective during a dip. The aim of this paper is to identify and explain the cause of rotor circuit transients developed during a voltage dip, and comment on the threat these particular transients impose on the converters used in SER drives. The focus of the study is on the mechanisms that cause rotor circuit transients. The control of SER electronics to limit the effects of these transients is beyond the scope of this project.

A considerable amount of work has been done on the mathematical modelling of SER drives for both steady state and transient condition [1-5]. However, very little information exists with regard to the response of a wound rotor induction motor to a disturbance such as a voltage dip. The transient currents developed by the rotor circuit during a voltage dip can cause rotor converter failure. Over-voltages as a result of these currents can cause breakdown across devices as voltage ratings are based on steady state operation over a limited speed range. The associated transient torques developed during these disturbances are considerable and can lead to the failure of gearboxes connected to the rotor shaft.

The rotor transients developed by a wound rotor induction motor are investigated for a range of three phase and single phase voltage dips. Measurements are conducted on a simplified SER circuit that assumes the rotor converters have no control over rotor currents developed during the voltage dip. Simulations performed using the Alternative Transients Program confirm the measured results and allow for a better understanding of the problems associated with SER drives and voltage dips.

2. SLIP ENERGY RECOVERY (SER)

The speed of a wound rotor induction motor can be

controlled by varying the rotor resistance and hence the slip of the machine. This is typically realised using external resistors connected to the rotor slip rings. By adding rotor resistance and increasing the operating slip, the speed of the motor can be reduced (Figure 1).

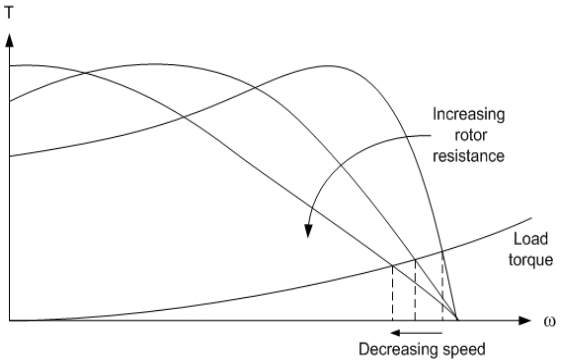

Figure 1: Torque/Speed characteristics for varying rotor resistance.

The disadvantage of achieving speed control by adding rotor resistance is that operating an induction motor at high slip is inherently inefficient. The power transferred across the air-gap of the machine is either dissipated as heat in the rotor resistance or transformed into mechanical power. For operation at less than one-half synchronous speed, more than half of the power crossing the air-gap is dissipated in the rotor windings and the external rotor resistors [6].

SER is an alternative approach to induction motor speed control. Modern SER drives consist of back-to-back voltage source converters which are positioned in the rotor circuit of a wound rotor induction motor (Figure 2). These converters decouple the mechanical and electrical rotor frequencies and thus circulate the rotor power back to the supply at the correct voltage and frequency. Converters are rated at slip power and control the torque-speed characteristics of the motor to achieve speed control. The stator terminals are connected to an infinite bus, which results in an almost constant airgap flux and a torque proportional to the mean DC link current [2].

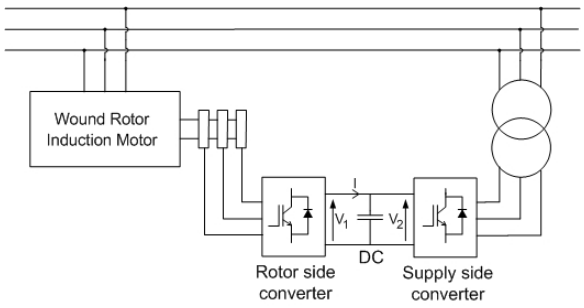

Figure 2: SER circuit

Another popular implementation of this principle is with doubly fed induction generators (DFIGs) which are becoming increasingly popular in wind power generation. These generators are able to supply power to the grid at constant voltage and frequency with variable rotor speed making them robust and more efficient than fixed frequency/speed wind generators [7].

Speed control using SER is achieved in exactly the same manner as using external rotor resistance, only the necessary resistance is synthesised using the back-to-back voltage source converters in the rotor circuit. The result is that the low speed efficiency of the induction motor is improved considerably as the slip power is returned back to the supply. Bidirectional power flow can be achieved which allows for regenerative braking and generation at both sub-synchronous and super-synchronous speeds [3, 5, 7].

Converters need only be rated at slip power which is typically 25 % of the total power of the system. IGBTs are rated according to the maximum voltage and maximum current for a particular operating slip and are thus not designed to ride through start-up or re-switching transients. Disturbances that result in large transient rotor currents and voltages in the order of magnitude of these disturbances can thus lead to IGBT failure.

The use of a crowbar across the rotor rings or a braking resistor across the DC bus have been used for protection purposes [2]. The use of a crowbar across the rotor rings is problematic from a mechanical perspective as its operation is associated with large transient torques, which if not sufficiently damped can result in excessive wear and premature failure of gearboxes.

3. VOLTAGE DIPS

Voltage dips are classified as a sudden reduction in the RMS supply voltage for a period of between 20 ms and 3 s of any or all phase voltages in a single or poly-phase supply. The duration of a voltage dip is the time measured from the moment the RMS voltage drops below 0.9 per unit of the declared voltage to when the voltage rises above 0.9 per unit of the declared voltage [8].

Voltage dips are typically caused by network faults. Fault currents result in large voltdrops across network impedances resulting in voltage reduction further down the network. Voltage dip parameters depend on the proximity of the fault and how quickly protection circuitry operates to clear the fault.

Faults resulting in voltage dips can occur within the plant or on the utility system. The dip condition will

last until the fault is cleared by a protection device, typically a fuse or substation breaker. The action of reclosers used by many utilities can cause multiple voltage dip conditions. It is important for customers to ensure critical/sensitive equipment is adequately rated and protected against disturbances such as voltage dips.

The majority of faults on a utility system are single line-to-ground faults [9]. Three phase faults are less common but are typically more severe. Industrial plants that make use of SER drives can experience poor power quality and may be subject to many voltage dips. Plants such as mines which have exposed power systems and are located in areas with high lightning flash densities may experience many severe dips on an annual basis.

4. SIMULATION

Simulations were performed using the Alternative Transients Program (ATP) [10] to complement and gain a better understanding of the motor behaviour over a range of different voltage dips. The Universal Machine (UM4) model of a wound rotor induction motor in ATP was used to predict the transient performance of the motor during the applied voltage dips. The UM4 model is versatile as it allows for interfacing between electrical, control and mechanical systems [11]. Furthermore the model can be modified to include non-linear effects such as saturation.

In ATP, the machine equations are solved in the d-q-0 reference frame using Park's transformation. For a detailed description of the formulation of the motor differential equations and the assumptions used refer to [10, 11]. This linear d-q model has been extensively used for studying motor transients whereby magnetic saturation and distribution effects in the rotor circuit have been neglected [12].

The characteristics of an induction motor depend primarily on the combined leakage inductance of the stator and the rotor and on the rotor resistance [6]. These characteristics are not constant and vary with the speed difference between the rotor and the rotating magnetic field in the air gap (the slip speed) [13]. Variation of rotor resistance is caused by eddy currents and skin effect in the rotor windings and variation of the leakage inductance is primarily due to magnetic saturation of the leakage flux paths [14].

Compared to a squirrel cage motor, skin effect and eddy currents in the rotor windings of a wound rotor induction motor are less significant and are thus ignored. However, during a transient event, such as start-up or a voltage dip, the stator and rotor leakage inductances are dominant variables and govern the way the motor behaves [6].

At no load, the rotor speed approaches synchronous speed and the rotor frequency is small. The rotor reactance at no load is small and the rotor resistance is the governing characteristic. A lower rotor resistance will result in a larger rotor current for a lower value of slip, resulting in more torque and a higher no load speed.

As the machine is loaded, the rotor leakage reactance increases as the rotor frequency increases. This causes the rotor currents to lag the emfs producing them and hence the maximum rotor current does not coincide with the maximum gap flux density [6]. The rotor leakage reactance increases the rotor impedance for the particular load condition, reducing the rotor current and establishing a phase angle between the gap flux and rotor current. The variation of this angle is responsible for the variation of torque under different load conditions. The maximum torque developed by an induction motor depends on the rotor leakage reactance only and the speed for maximum torque is dependant on the ratio of the rotor resistance to rotor leakage reactance. Variation of the rotor resistance will only change the slip at which the maximum torque occurs.

The leakage reactances of an induction motor can vary significantly during a transient event such as a voltage dip. The transient currents developed during a dip result in large values of slot leakage flux in both the stator and rotor slots. This flux tends to saturate the teeth of the motor. As a result, the leakage inductances of the motor, which are typically modelled to be constant, become functionally dependant on the motor currents [15].

There are several components of leakage flux present in an induction motor, namely slot, zig-zag, belt, skew, and end winding leakage [6, 15]. These fluxes (except for the end winding leakage) are saturable quantities as the major portion of their paths travels through iron. Saturation of the iron in the induction motor is a complicated process and is thus difficult to model. In practice, leakage path saturation takes place in either the stator or rotor teeth and according to [15], sufficient accuracy can be obtained by modelling only one of the two leakage path saturation effects. Calculation of the combined leakage inductance can be accomplished by analytical means however, in the absence of design data, the leakage saturation effect is best measured by means of a locked rotor test [15].

In this study, the motor under test did not demonstrate significant saturation of the leakage flux paths. This is the case because the motor has a relatively large airgap. The reluctance of the airgap dominates the total reluctance of the magnetic circuit in the machine and results in an almost linear leakage inductance. Machines that are tubular and

have small airgaps with respect to their stack lengths will exhibit greater saturation of the leakage parameters [15].

The measured motor parameters are presented in Table 1 and were obtained following standard no load and locked rotor tests. The combined stator and rotor leakage inductance obtained from the locked rotor tests is shown in Figure 3.

Table 1: Equivalent circuit parameters (referred to the stator)

R_{stator}	0.705 Ω
L_{stator} (unsat)	0.011 H
L_{mutual}	0.372 H
R_{rotor}	1.024 Ω
L_{rotor} (unsat)	0.011 H

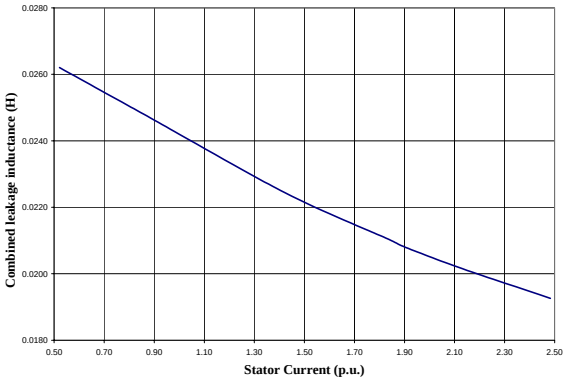

Figure 3: Locked rotor leakage inductance

To show the effect of saturation in the simulation, it was first assumed that the leakage inductances were constant. The leakage inductances input into ATP were selected for rated current operation. The results of this simulation confirmed that the d-q model was sufficient to model the transients developed by the rotor circuit during a dip. For larger magnitude dips however, the resulting time constants and current magnitudes were inaccurate. A closer correlation was obtained with measured results by selecting a constant leakage inductance that corresponded to the transient currents developed during the voltage dip (i.e. at 2.5 times rated current). In this case, although the rotor transients matched the measured cases, the behaviour of the motor over the normal range of operating slip speeds was erroneous as the value of leakage inductance was too small for normal operating currents.

To include the effects of saturation, the leakage inductances for both stator and rotor were separated into saturable and unsaturable quantities. Saturation was modelled as a function of stator and rotor currents and was accomplished using the current dependant non-linear inductors found in ATP. These inductors were added externally to the UM model in the simulation as shown in figure 4. The inclusion of the non-linear parameters resulted in an accurate simulation of the induction motor over a range of voltage dip parameters. The results of the simulations are presented and discussed in Section 7.

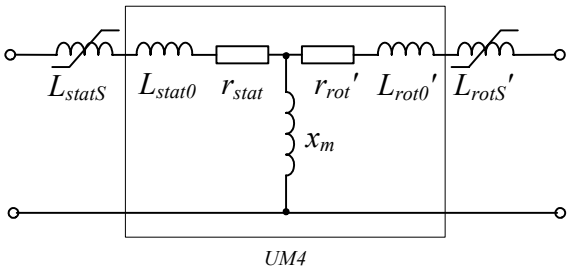

Figure 4: Equivalent circuit with saturable and unsaturable leakage inductances

The induction motor used in this study showed minimal saturation of the leakage parameters so the inclusion of these effects in the simulation was not particularly significant. This may not be the case for motors that are typically used in SER applications. The inclusion of saturation effects may thus be necessary for such a simulation.

5. WOUND ROTOR INDUCTION MOTOR REPONSE TO VOLTAGE DIPS

A voltage dip at the supply terminals of an induction motor will produce transient currents and transient torques depending on the severity of the dip and on the motor parameters [6]. Transients can be separated into those generated at the instant of the voltage dip and those generated at the instant of voltage recovery.

The sudden reduction of voltage at the supply terminals of a wound rotor induction motor will have the following consequences:

1. The stator voltage governs the stator flux conditions in the machine. At the instant of a voltage dip, the stator voltage attempts to enforce a new stator flux condition in the motor. The developed emf that opposes this voltage (neglecting the stator resistance voltdrop) and develops the stator flux is given by the equation [6]:

$$E_1 = 4.44 K_{w1} f T_1 \Phi_m$$

where: E_1 = *RMS* stator emf per phase
K_{w1} = stator winding factor
f = stator supply frequency
T_1 = stator turns per phase
Φ_m = peak mutual flux

The mutual flux component of the total stator flux will be similarly affected. The change in mutual flux as developed by the stator is thus

dependant on the magnitude of the voltage dip.

2. The principle of superposition applies and the dip in the supply voltage can be considered as a sudden application of a negative voltage at the terminals of the machine. A short circuit condition will result if this negative voltage is equal to the applied terminal voltage and is obviously the worst case scenario.

3. The magnitudes of the currents developed at the instant of a voltage dip depend primarily on the flux linked by the windings at that instant. If at the instant of the voltage dip the flux linkage for a particular winding is at a maximum, the current magnitudes developed by the winding will be worst case. If there is no flux linking the winding at the instant of a dip, the transient currents developed are insignificant. This fact was confirmed during the single phase tests. Figure 5 shows how the flux linkage of a particular winding will affect the transient currents developed in that winding. For a three phase dip there is three times more chance that any winding will link maximum flux.

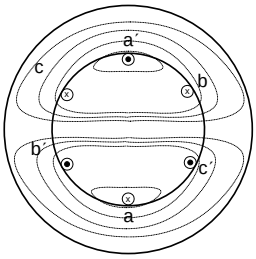

A voltage dip at the instant winding *a* links maximum flux results in the worse case transient current.

The stator currents must respond in an attempt to change the flux linkage of winding *a*.

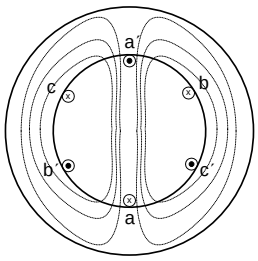

A voltage dip at the instant winding *a* links no flux will have no significant effect.

Figure 5: Instantaneous flux linkages

4. Two pairs of transient currents are developed by the machine at the instant of the dip – a constant amplitude AC current and a decaying DC current. A DC current vector that is equal in magnitude but opposite in sign to the instantaneous value of the three phase rotating current vector at the instant of the dip must be developed by the motor windings [16]. This DC current remains stationary in space but decays with time according to the combined stator and rotor leakage reactances.

5. The theorem of constant flux linkage states that the flux linking the stator and rotor windings in the machine cannot instantaneously change. The stator currents developed at the instant of the voltage dip will attempt to demagnetise (reduce the mutual flux) the machine. This forces the rotor circuit to respond and produce equal and opposite currents to maintain the flux linkages of the windings at that instant. This effect results in large transient currents developed in the rotor circuit. These rotor currents will also consist of AC and DC components as for the stator currents.

6. The rotor windings have rotational speed and thus the flux fixed to the stator induces voltages on the rotor side. The induced voltages will result in transient currents in the rotor circuit with a frequency dependant on the speed of the rotor.

7. The transient rotor currents and stator currents developed as a result of the voltage dip will generate large transient torques [16, 17]. Depending on the severity of the dip, the motor characteristics and the added external rotor resistance, the developed transient torque can approach direct-on-line starting torques for those particular parameters.

8. In a short-circuited squirrel cage motor the transient rotor currents and voltages have little consequence; however in the case of SER drives with rotor circuit converters based on limited steady state ratings, the resulting transient rotor voltages and currents can cause flashover or device failure respectively.

The response of an induction motor to voltage recovery can generate even larger transients than at the instant of a voltage dip. These transients depend primarily on the flux conditions within the motor at the time of recovery and on the rotor speed. These can be identified as re-switching transients similar to those developed when a machine changes from one steady state operating condition to another (e.g. star-delta switching) [12, 16].

The response of a motor to voltage recovery is as follows:

1. The mechanisms that cause transients at the instant of voltage recovery are complicated and depend on the flux conditions within the machine at that time. Effects such as skin effect in the rotor windings, the reaction of the core due to the rapid rise in flux and mechanical considerations inherent in the design of the shaft and windings complicate the process [6, 16].

2. The theorem of constant flux linkage plays an important role in the understanding of the transients generated during voltage recovery. At the instant of voltage recovery the flux linkage must remain constant. The severity of the transients generated is thus dependant on the flux conditions within the machine at that instant.

3. It takes time for magnetic energy stored in a motor to dissipate. Trapped flux will continue to induce both rotor and stator emfs dependant on the size and parameters (time constants) of the motor.

4. Upon voltage recovery, phase differences may exist between the supply voltage and induced emfs as a result of trapped flux. If phase opposition occurs, the transient currents may be very severe. Thus the amount of stored energy in the motor and the position of the rotor which affects the flux linkage, will affect the transients developed in both the stator and rotor circuits at the instant of voltage recovery.

6. TEST CIRCUIT

A simplified SER circuit was used for test and simulation purposes. Rotor transients developed by the motor during a voltage dip are injected into the DC bus via the rotor side converter. In this study, the converter is simplified to a three phase diode bridge rectifier (the anti-parallel diodes of the rotor side converter) connected to a DC bus capacitor and a rotor resistor (Figure 6). The resistor is sized such that the motor operates at the required slip for a given load condition.

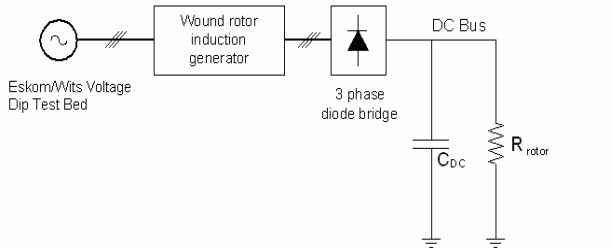

Figure 6: Simplified SER test circuit

Converter control circuitry can limit conduction of the IGBTs. However, it cannot control conduction of the anti-parallel diodes when transient currents are developed by the rotor windings during a voltage dip. The circuit in Figure 3 assumes that the rotor circuit converters have no control over the rotor current during a dip. If the converters can maintain some control of the rotor current, a more detailed investigation would be required.

The flux level in a motor is dependant on the stator voltage. At the instant of a voltage dip, the stator voltage will impose a new stator flux condition in the motor. In order for the balance of mmf to be maintained at the instant of the voltage dip, the rotor circuit has to respond to sustain the instantaneous flux linkage of the windings. As a result, the currents developed by the rotor circuit may have direction opposite to the previous direction and hence flow through the free-wheeling diodes rather than the IGBTs. The theorem of constant flux linkage [6] governs how the rotor circuit will respond and hence it is the author's belief that it will be difficult for converters to limit the rotor currents by adopting complex control strategies. This could be a topic for future research.

Measurements and simulations were conducted on a 19 kW 4 pole wound rotor induction motor with specifications given by Table 2.

Table 2: Wound rotor induction motor parameters

Rated power	19 kW
V_{stator}	500 V
I_{stator}	25 A
V_{rotor}	270 V
I_{rotor}	44 A
Stator/rotor connection	delta/star
Transformer ratio	1.95/1
Moment of inertia	0.3 kg.m^2

Balanced three phase and single phase dips were applied using the Eskom/Wits Voltage Dip Test Bed. A variety of dips were chosen to show the effects of different voltage dip parameters on the developed rotor circuit transients.

7. MEASUREMENT

A range of voltage dip parameters were chosen to explain and quantify transients developed by the rotor circuit. These included single phase and three phase dips. The motor under test was run at varying load conditions and at different speeds typically associated with SER applications.

Measurements were conducted using the Eskom/Wits Voltage Dip Test Bed. The resulting stator current, rotor current and DC bus voltage were recorded to determine the response of the rotor circuit of the motor to the applied voltage dips. Results proved to be repeatable.

7.1. Three phase dips

Table 3 shows selected results of a series of balanced three phase dips. In this test, voltage dips of magnitude 0.4 p.u. were applied for different dip

durations. A rotor resistance of 1.2 ohms was chosen such that at full load, the motor was operating at approximately 0.2 p.u. slip. A DC capacitance of 3.3 μF was chosen such that the full load steady state voltage ripple was limited to under 10 %.

A constant load torque was applied to the motor for the duration of the test. The DC bus current was proportional to the DC bus voltage as a result of the rotor resistance across the DC bus.

Table 3: Balanced three phase 0.4 p.u. dip results

Dip duration (ms)	Supply cycles	Maximum V_{dc}/I_{dc} (p.u.)
10	0.5	3.3
20	1.0	1.9
30	1.5	3.1
40	2.0	2.0
50	2.5	2.9
60	3.0	2.2
70	3.5	2.7
80	4.0	2.6
90	4.5	2.3
100	5.0	2.7
150	7.5	2.0
200	10.0	2.7
250	12.5	2.0

Table 4 shows results of the same test conditions only the dips of magnitude 0.6 p.u. were applied.

Table 4: Balanced three phase 0.6 p.u. dip results

Dip duration (ms)	Supply cycles	Maximum V_{dc}/I_{dc} (p.u.)
10	0.5	4.0
20	1.0	2.3
30	1.5	3.7
40	2.0	2.4
50	2.5	3.5
60	3.0	2.7
70	3.5	3.1
80	4.0	3.1
90	4.5	2.9
100	5.0	3.3
150	7.5	2.3
200	10.0	3.7
250	12.5	2.3

The maximum rotor current and voltage for balanced three phase dips occur at the instant of voltage recovery. The voltage dip magnitude and duration are the most significant parameters that determine the maximum rotor transients. Voltage dips with duration of whole cycles cause minimum transients and dips with duration of half cycles cause maximum current and torque transients. Perhaps the most interesting result is the fact that shorter dips produce significantly larger transients than longer dips. It appears the flux held stationary with respect to the stator windings introduces substantial phase differences between the applied voltage and induced emf in the motor windings. The severity of this phenomenon is dependant on the time constant of the DC component of flux.

Figures 8 and 9 show a comparison between the simulated and measured DC bus voltages for a 100 ms 0.4 p.u. balanced three phase dip as shown in Figure 7. These waveforms are typical of the results for all balanced three phase dips.

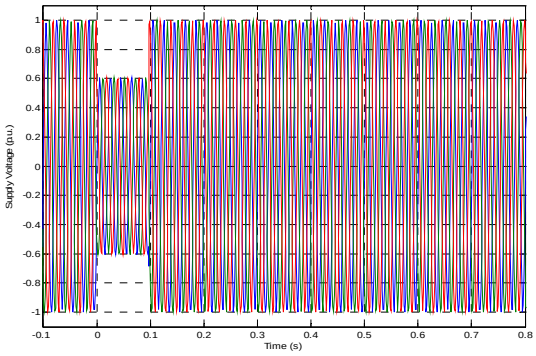

Figure 7: 100 ms 0.4 p.u. balanced three phase dip

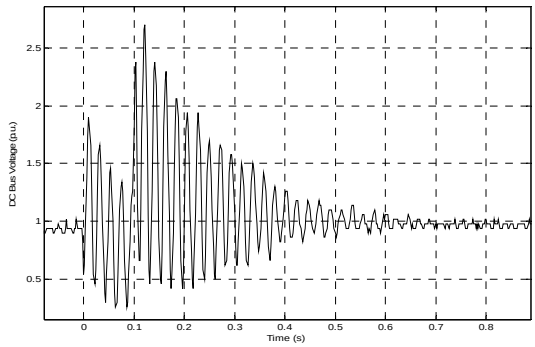

Figure 8: Measured DC bus voltage (p.u.)

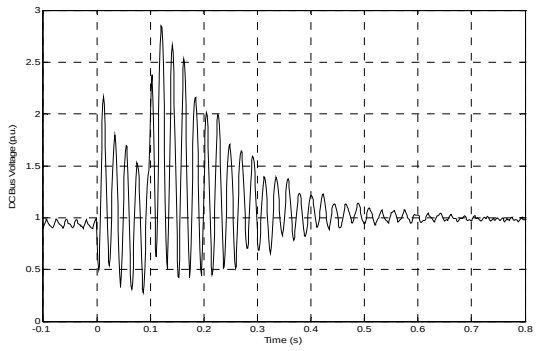

Figure 9: Simulated DC bus voltage (p.u.)

7.2. Single phase dips

The current transients generated as a result of a single phase dip depend primarily on the flux linking that particular phase winding at the instant of the dip (as discussed in Section 5). Table 5 shows a selection of single phase dip results to illustrate the recorded results.

Table 5: Single phase dip results

Dip magnitude (p.u.)	Dip duration (ms)	Flux linkage	Maximum V_{dc}/I_{dc} (p.u.)
0.4	10	Min	1.5
0.4	10	Max	2.8
0.6	10	Min	1.8
0.6	10	Max	3.7
0.4	50	Max	2.5
0.4	100	Max	2.5
0.4	250	Max	2.6

For single phase dips the voltage dip duration is not as significant as for three phase dips. The maximum transients are produced at the instant of the voltage dip and not at the point of recovery. The magnitude of the voltage dip and the instantaneous flux linkage of the phase winding that experiences the dip are the significant parameters and determine the response of the rotor circuit.

Figures 11 and 12 show a comparison between the simulated and measured DC bus voltages for a 100 ms 0.4 p.u. single phase dip as shown in Figure 10. Again, these waveforms are typical of the results for all the single phase dips.

A comparison of loading conditions reveals that the magnitude of the rotor transients developed during a voltage dip does not depend significantly on the load torque developed by the motor at that time. A motor that runs at rated load during a voltage dip exhibits similar magnitude rotor currents compared to an unloaded case. The stator winding flux linkage does not change significantly throughout the range of rated operation of the induction motor [6] and it is this flux linkage that determines how the rotor circuit must respond at the instant of the voltage dip.

Tests were performed to see how operation at different slip speeds altered the response of the rotor circuit to a dip. The rotor resistance synthesised by the converters determine the dynamic response of the motor to a voltage disturbance. This resistance governs the speed for a particular load condition. The greater the rotor resistance the more damped the transient currents injected into the DC bus appear to be. This is most obvious for the three phase dip case at voltage recovery.

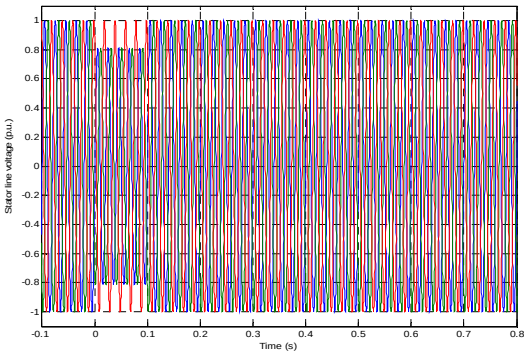

Figure 10: 100 ms 0.4 p.u. single phase dip

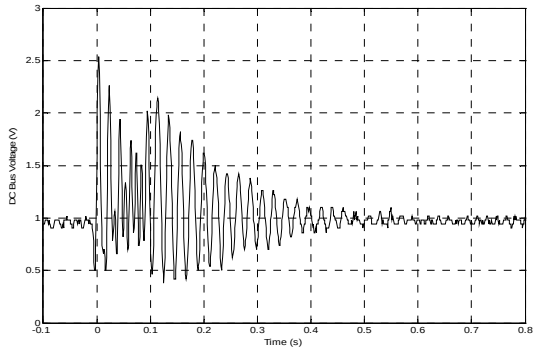

Figure 11: Measured DC bus voltage (p.u.)

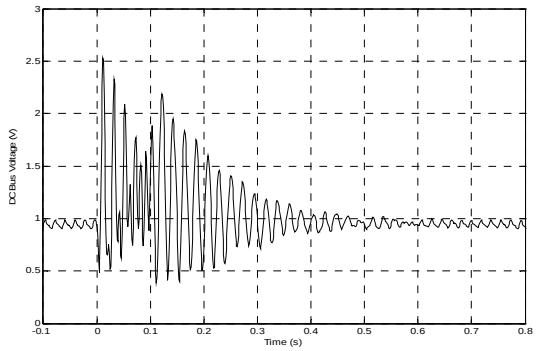

Figure 12: Simulated DC bus voltage 100ms 0.4 (p.u.)

Longer duration dips were performed on the test circuit, however, the motor tended to slow down substantially. This result meant that the transients developed at voltage recovery were not representative of what might be anticipated in typical SER applications, where the motors tend to drive high inertia loads.

The IGBTs and free-wheeling diodes used in the rotor converters are typically rated at 2 p.u. voltage and current for a limited steady state operating range. Over-currents and over-voltages of well over these ratings have been measured for relatively moderate dips in this study.

The size of the DC bus capacitance has an important influence on the magnitude of the DC bus transients during a voltage dip. A larger capacitance reduces the rotor transients considerably. The tendency to

use smaller capacitance in the DC bus of modern converters limits the effect of the capacitance in the reduction of rotor transients during a dip.

8. COMPARISON OF MEASURED AND SIMULATED RESULTS

The d-q model proved to be adequate to model the dynamic response of the rotor circuit to a voltage dip with results comparing well to the measured cases. The inclusion of saturable leakage inductances improved the simulation results especially with regard to the magnitude and time constants of the developed current transients.

Matching the exact instant in time (point on wave) the voltage dip occurs is very important for the simulation as a period as short as 1 ms produces very different results. The same is true for voltage recovery. This requires that the correct steady state parameters have been included in the model such that the power factor and rotor speed are very accurate.

The use of a low inertia load was perhaps not an entirely accurate representation of a SER application as the motor under test slowed down substantially for longer duration dips. Simulation of a motor loaded with an extremely high moment of inertia, did however exhibited similar but reduced electrical transients as those measured in the test case.

9. RECOMENDATIONS

The following may be considered to limit the transient currents injected into the DC bus by the rotor circuit (or limit the effects of these currents):

1. Driving the DC bus voltage up during a dip may limit the current transient injected into the DC bus. By effectively synthesising a larger rotor resistance, the machine parameters are altered such that the currents injected into the DC bus are reduced during the dip and at voltage recovery. This would however require that converter IGBTs be rated at larger voltages.

2. By switching an external (bypass) resistor connected in parallel to the DC bus using a controlled switch, the transients generated by the rotor circuit during a dip can be significantly damped (this will ensure the supply side converter is removed from the circuit). Care must be taken such that the resistance is sized so both electrical and mechanical transients are reduced to acceptable levels.

3. Adopting a control strategy that allows the rotor circuit converters to control the rotor currents of the motor during a voltage dip.

10. CONCLUSION

The objective of this paper has been to gain a better understanding of the problems associated with the effect of voltage dips on SER drives and to explain the rotor circuit response to voltage dips from the machine's perspective. The mechanism of constant flux linkage plays an important role in the magnitude of the currents and voltages produced in the rotor circuit. Trapped flux present in the motor during a voltage dip appears to play a significant role in the production of transient currents, especially for shorter duration dips.

It is evident that voltage dips are cause for concern with regard to SER rotor converters. Relatively moderate dips can cause current and voltage electrical transients of well over 2 p.u. The scalability of these results to larger motors used in SER applications can only get worse as these motors typically exhibit very small rotor resistances and long time constants.

The most surprising result of this research is the fact that shorter duration three phase dips of a half cycle duration produce considerably larger transients than longer duration dips. These short duration dips can be caused by fuse clearance of network faults.

The above analysis assumes that the equivalent circuit of Figure 3 is valid during the dip. If the converters maintain control over the rotor current during the dip then a more detailed investigation would be required.

REFERENCES

[1] E. Akpinar, P. Pillay, Modeling and performance of slip energy recovery induction motor drives, *IEEE Transactions on Energy Conversion*, v 5, n 1, Mar, 1990, pp 203-210.

[2] I. Çadirci, G. Akçam, M. Ermis, Effects of instantaneous power-supply failure on the operation of slip-energy recovery drives, *IEEE Transactions on Energy Conversion*, v 20, n 1, Mar, 2005, pp 7-13.

[3] R. Pena, J. C. Clare, G. M. Asher, Doubly fed induction generator using back-to-back PWM converters supplying an isolated load from a variable speed wind turbine. *IEE Proceedings: Electric Power Applications*, v 143, n 5, Sep, 1996, p 380-387.

[4] J. B. Ekanayake, L. Holdsworth, X. Wu, N. Jenkins, Dynamic modeling of doubly fed induction generator wind turbines, IEEE Transactions on Power Systems, v18, n2, May 2003, pp803-809.

[5] I. Çadirci, M. Ermis, Double-output induction generator operating at subsynchronous and supersynchronous speeds: steady-state performance optimisation and wind-energy

recovery, IEE Proceedings, Part B: Electric Power Applications, v 139, n 5, Sep, 1992, pp 429-442.
[6] M. G. Say, Alternating Current Machines 4th ed, Pitman, London, 1976.
[7] V. T. Ranganathan, R. Datta, Variable-speed wind power generation using doubly fed wound rotor induction machine - A comparison with alternative schemes, IEEE Transactions on Energy Conversion, v17 n 3 Sept 2002 pp 414-421.
[8] NRS. Minimum standards, NRS 048-2 (Electricity Supply – Quality of Supply). NRS, 1996.
[9] M. F. McGranaghan, D. R. Mueller, M. J. Samotyj, Voltage sags in industrial systems, IEEE Transactions on Industry Applications, v 29, n 2, Mar-Apr 1993, pp 397-403.
[10] Leuven EMTP Centre, Alternative Transients Program Rule Book, Leuven, Belgium, 1992.
[11] H. K. Lauw, W. S. Meyer, Universal machine modelling for the representation of rotating electrical machinery in an electromagnetic transients program, *IEEE Transactions on Power Apparatus and Systems*, v PAS-101, n 6, Jun 1982, pp 1342-1351.
[12] J. Reynaud, P. Pillay, Reclosing transients in induction machines including the effects of saturation of the magnetizing branch and a practical case study, *IEEE Transactions on Energy Conversion*, v 9, n 2, Jun 1994, pp 383-389.
[13] G. J. Rogers, D. Shiromohammadi, Induction machine modelling for electromagnetic transient program, *IEEE Transactions on Energy Conversion*, v EC2, n 4, Dec 1987, pp 622-628.
[14] S. D. Sudhoff, D. C. Aliprantis, B. T. Kuhn, P. L. Chapman, An induction machine model for predicting inverter-machine interaction, *IEEE Transactions on Energy Conversion*, v 17, n 2, Jun 2002, pp 203-210.
[15] T. A. Lipo, Modelling and simulation of induction motors with saturable leakage reactances, IEEE Transactions on Industry Applications, v IA-20, n 1, Jan/Feb, 1984, pp 180-189.
[16] P. K. Kovacs, Transient Phenomena in Electrical machines, Elsevier, New York, 1984.
[17] J. C. Das, Effects of momentary voltage dips on the operation of induction and synchronous motors, *IEEE Transactions on Industry Applications*, v 26, n 4, Jul-Aug, 1990, pp 711-718.

Appendix A

Simulation

This chapter presents the models used in the ATP simulations that make up the slip energy recovery test circuit as presented in the paper.

A.1 Dynamic modelling of induction motors

The traditional per phase equivalent circuit is only valid for steady state analysis of induction motors. In order to adequately model and describe the behaviour of an induction motor during a voltage dip, the dynamic motor model equations are necessary. The UM4 (wound rotor induction motor) model in ATP was chosen for the simulations as it adequately describes the dynamic behaviour of the wound rotor induction motor under transient conditions such as a voltage dip.

Generalised machine theory, provides a very powerful tool for studying electrical machines under transient conditions. This theory is most applicable for modelling transient conditions whereby large currents and torques are developed by the machine (i.e. starting conditions, fault conditions and re-switching conditions). Generalised machine theory was developed to model synchronous, induction and DC motors as all electrical machines operate under the same fundamental principle – the tendency of two magnets to align themselves [1]. The UM (universal machine) model used in EMTP–ATP is based on this theory and allows for easy interfacing between electrical, control, and mechanical systems and was the obvious choice for modelling wound rotor induction motors [2].

A.2 d-q fundamentals

The dynamic coupled circuit equations of an induction motor are complex as they depend on differential equations with variable coefficients [3]. As the rotor moves, the flux linking the rotor and stator coils will change because of the relative movement between the axes of the rotor and stator. The d-q model eliminates this complexity by applying complex vector representations of the machine variables such that the machine equations reduce to a manageable form. In ATP, the machine equations are solved in the d-q-0 reference frame using Park's transformation.

The following section introduces the basic theory of the dynamic space vector approach to modelling of an induction motor as used in EMTP–ATP.

In an induction motor, the three phase stator windings will produce a sinusoidally distributed mmf in the airgap. Assuming a uniform airgap and neglecting the effects of space harmonics, the magnetic flux will also be sinusoidal. Consider the following instantaneous stator currents which are displaced 120° apart:

$i_{SA}(t)$ instantaneous current in phase A
$i_{SB}(t)$ instantaneous current in phase B
$i_{SC}(t)$ instantaneous current in phase C

These three currents are added vectorially to obtain a resultant current space vector [4]:

$$\vec{i}_S(t) = i_{SA}(t) + i_{SB}(t)e^{-j2\pi/3} + i_{SC}(t)e^{-j2\pi/3} \qquad \ldots\text{A.1}$$

For balanced three phase currents, $\vec{i}_S$ rotates with constant angular velocity and constant magnitude. Figure A.1 shows this relationship.

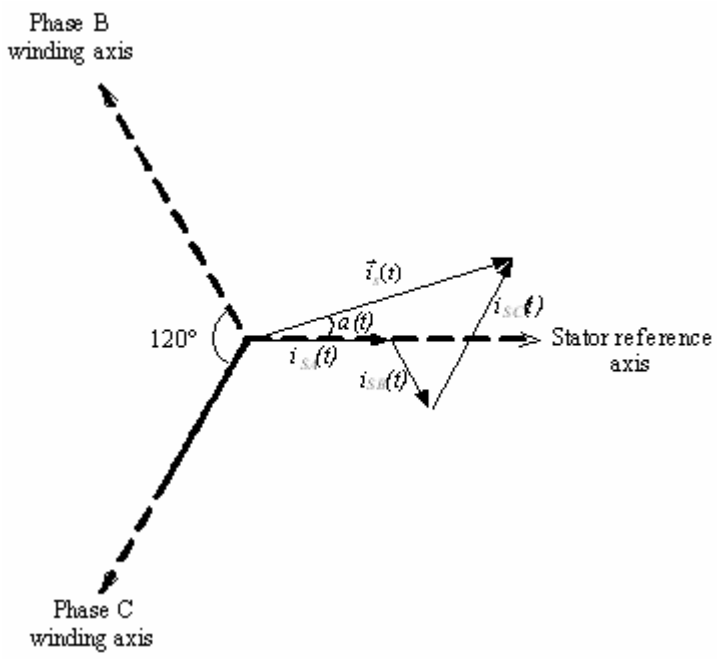

Figure A.1: Stator current space vector and stator phase currents [4]

The three phase variable representation of the stator currents has been transformed into an equivalent two phase representation as shown in the figure. The transformation is reversible and each phase quantity can be calculated from the space vector. This transformation is equally valid for the voltage and flux linkage equations and is applied to the rotor circuit variables in the same manner. The development of the voltage and flux linkage equations for induction motors can be found in [5].

The voltage equations of the induction motor are written for the stator and rotor phases in terms of self and mutual inductances. As the rotor moves, the mutual inductances between the rotor and stator coils will change, because the angle between the axes of the rotor and stator changes. To eliminate the time-varying inductances, it is necessary to transform both stator and rotor quantities into a common reference frame such that the equations become manageable. This is achieved using vector rotation or the Park transformation.

The stator and rotor voltage space vector equations are as follows [4]:

$$\vec{v}_S(t) = \vec{i}_S(t)R_S + \frac{d\vec{\varphi}_S(t)}{dt} \qquad \ldots \text{A.2}$$

$$\vec{v}_R(t) = \vec{i}_R(t)R_R + \frac{d\vec{\varphi}_R(t)}{dt} \qquad \ldots \text{A.3}$$

where $\vec{v}_S(t)$ = rotating stator voltage space vector

$\vec{i}_S(t)$ = rotating stator current space vector

R_S = stator winding resistance

$\vec{\varphi}_S(t)$ = rotating stator flux linkage space vector

$\vec{v}_R(t)$ = rotating rotor voltage space vector

$\vec{i}_R(t)$ = rotating rotor current space vector

R_R = rotor winding resistance

$\vec{\varphi}_R(t)$ = rotating rotor flux linkage space vector

The stator voltage equation is described in stator coordinates and the rotor voltage equation in rotor coordinates. The relation between stator and rotor coordinates is given by:

$$\vec{x}_S(t) = e^{j\theta_R}\vec{x}_R(t) \qquad \ldots \text{A.4}$$

where θ_R = the rotor angle referred to the stator reference

The stator ($\vec{\varphi}_S(t)$), rotor ($\vec{\varphi}_R(t)$), and mutual flux linkages ($\vec{\varphi}_M(t)$) are given by [5]

$$\vec{\varphi}_S(t) = L_S\vec{i}_S(t) + L_M\vec{i}_R(t)e^{j\theta_R} = (L_{S\lambda} + L_M)\vec{i}_S(t) + L_M\vec{i}_R(t)e^{j\theta_R} \qquad \ldots \text{A.5}$$

$$\vec{\varphi}_R(t) = L_M\vec{i}_S(t)e^{-j\theta_R} + L_R\vec{i}_R(t) = L_M\vec{i}_S(t)e^{-j\theta_R} + (L_{R\lambda} + L_M)\vec{i}_R(t) \qquad \ldots \text{A.6}$$

$$\vec{\varphi}_M(t) = L_M\vec{i}_S(t) + L_M\vec{i}_R(t)e^{j\theta_R} \qquad \ldots \text{A.7}$$

where L_M = magnetising inductance

L_S = stator inductance

L_R = rotor inductance

$L_{S\lambda}$ = stator leakage inductance

$L_{R\lambda}$ = rotor leakage inductance

By applying the vector rotation transformation the rotor quantities can be referred to stator such equations A.2 and A.3 become:

$$\vec{v}_S(t) = \vec{i}_S(t)R_S + \frac{d\vec{\varphi}_S(t)}{dt} \quad \ldots \text{A.8}$$

$$\vec{v}_R^S(t) = \vec{i}_R(t)R_R + \frac{d\vec{\varphi}_R^S(t)}{dt} - j\omega_R\varphi_R^S \quad \ldots \text{A.9}$$

where ω_R = rotor speed

The flux linkages referred to the stator reduce to:

$$\vec{\varphi}_S(t) = L_S\vec{i}_S(t) + L_M\vec{i}_R^S(t) \quad \ldots \text{A.10}$$

$$\vec{\varphi}_R(t) = L_M\vec{i}_S(t) + L_R\vec{i}_R^S(t) \quad \ldots \text{A.11}$$

$$\vec{\varphi}_M(t) = L_M\vec{i}_S(t) + L_M\vec{i}_R^S(t) \quad \ldots \text{A.12}$$

Thus by reducing the phase variables into a two axis equivalent (d-q) and by defining a common reference frame, the machine equations are readily solvable. The d-q variables can then be transformed back into their phase equivalent quantities.

For a detailed explanation of the dynamic machine equations and d-q analysis, refer to [1, 2, 5].

A.3 Slip energy recovery test circuit

The following section includes the test circuit as used in the ATP simulations to model the simplified SER circuit as discussed in the paper. The various components that make up the simulation are presented and the choice of each is discussed.

Figure A.2 shows the simulation test circuit.

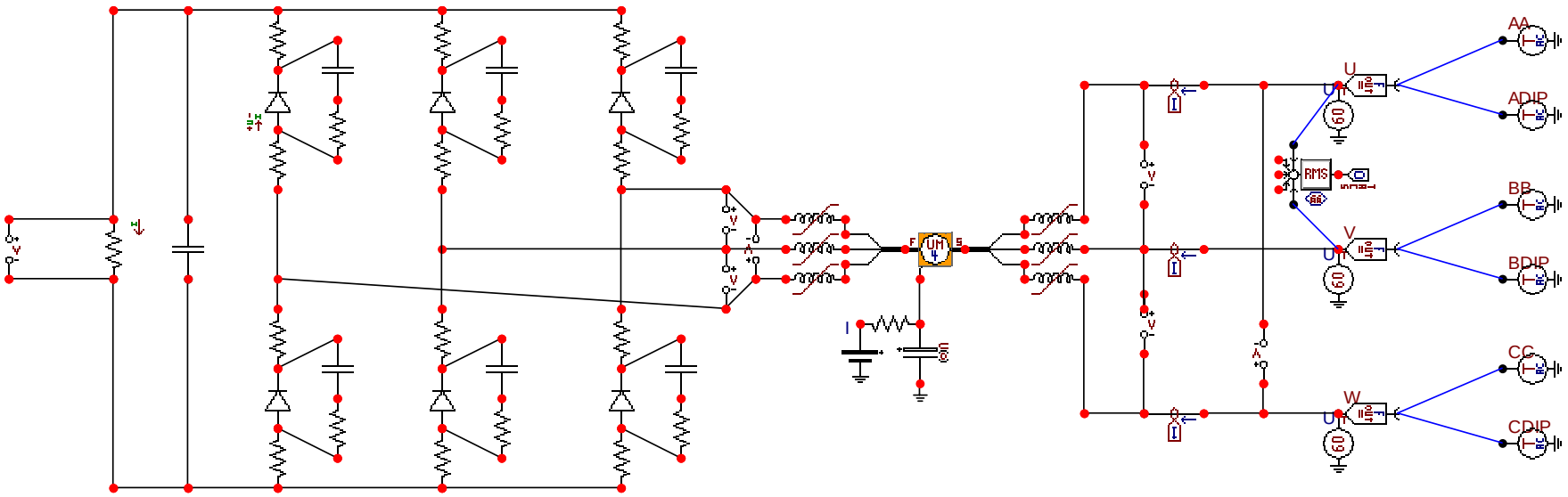

Figure A.2: Simulation test circuit

A.3.1 Leakage inductance saturation

To include the effects of saturation, the leakage inductances for both stator and rotor were separated into saturable and unsaturable quantities. Saturation was modelled as a function of stator and rotor currents and was accomplished using the current dependant non-linear inductors found in ATP (type 98) [2]. These inductors were added externally to either side of the UM4 model in the simulation as shown in Figure A.2. The inclusion of the non-linear parameters resulted in a more accurate simulation of the induction motor over a range of voltage dip parameters (especially for large magnitude dips). A detailed explanation of the effect of leakage inductance saturation is included in the paper.

A.3.2 Controlled voltage source

The controlled three phase supply to the induction motor was achieved using three TACS type 60 sources [2]. The combination of two type 14 TACS AC sources of equal phase but of opposite magnitude allowed for the synthesis of a voltage dip in any phase (Refer to Figure A.2). The duration and magnitude of the voltage dip at the terminals of the motor could thus be controlled using these sources.

The RMS line voltage at the stator terminals was measured using a TACS device 66 RMS meter.

A.3.3 Diode bridge model

The ideal diode (switch type 11 in ATP) model was used for the diode bridge connected to the rotor circuit. A snubber circuit across each diode was included with industry standard snubber values (capacitance = 0.1 μF; resistance = 47 Ω). The inclusion of the snubbers improved the rotor voltage waveforms to resemble those measured during the

tests. The inclusion of the snubber circuit did not seem to affect the rotor currents injected into the DC bus significantly. A symmetry resistance of 0.001 Ω was positioned either side of each diode in the circuit as ATP can experience problems with non linear devices. These resistors are small enough not to affect the simulation results.

A.3.4 Induction motor load model

The mechanical loading of the induction motor in ATP is achieved using an equivalent electrical circuit model. In this case as only constant load conditions were measured which required the inclusion of a capacitance at the motor load terminal in ATP. This capacitance was sized according to the moment of inertia of the coupled induction motor and DC generator. The negative DC source connected to the UM4 model represents the constant torque required by the load and hence controls the torque developed by the motor.

The resistance positioned across the DC bus controls the speed at which the induction motor runs for the given load torque condition.

A.3.5 Simulation comments

The UM4 motor model proved to be adequate to model the dynamic response of the rotor circuit to a voltage dip with results comparing well to the measured cases. The inclusion of saturable leakage inductances improved the simulation results especially with regard to the magnitude and time constants of the developed current transients.

Matching the exact instant in time (point on wave) the voltage dip occurs was very important for the simulation as a period as short as 1 ms produces very different results. The same was true for voltage recovery. This required that the correct steady state parameters had been included in the UM4 model such that the power factor and rotor speed were accurate.

A.4 Simulation results

The following section includes the simulated results from a 0.4 p.u. balanced three phase and a 0.4 p.u. single phase dip as presented in the paper. From an early stage the simulations confirmed many interesting results:

1. The maximum transients developed by the rotor circuit for a single phase dip are at the instant of the voltage dip. For three phase dips, the maximum transients occur at voltage recovery.

2. For balanced three phase dips, shorter dips produce larger rotor transients depending on the time of recovery. Dips of half cycle duration produce the largest rotor transients.

3. The stator winding flux linkage determines the response of the rotor circuit to a voltage dip. The greater the flux linkage, the greater the transients developed by the rotor circuit to maintain the flux within the motor.

4. The operating load condition of the motor is not as significant as was first anticipated. A motor running at no load produces transients of similar magnitude to that of a fully loaded machine. This confirms the fact that it is the stator flux linkage that is the most significant factor that determines the rotor response to a voltage dip (the stator flux linkage remains relatively constant over the operating range of the motor [6]).

5. The larger the DC bus capacitance, the less severe the rotor transients and transient torques appear to be.

6. A larger rotor resistance will dampen the response of the motor to a voltage dip. Running the machine at larger slip reduces the rotor transients developed by the wound rotor induction motor.

7. Simulation of a larger wound rotor induction motor produced similar results compared to the smaller motor case. Waveform signatures are similar depending on the point at which the dip is initiated.

A.4.1 Three phase results

The following results present a simulated 0.4. p.u. 100 ms balanced three phase dip. This case is representative of all the three phase dips. All the simulation parameters are the same as presented in the paper. The rotor side parameters were referred to the stator quantities in ATP (this included the delta/star conversion and the stator/rotor transformer ratio). The simulated data was then input into MATLAB and processed as required. Good correlation was obtained in comparison to the measured results.

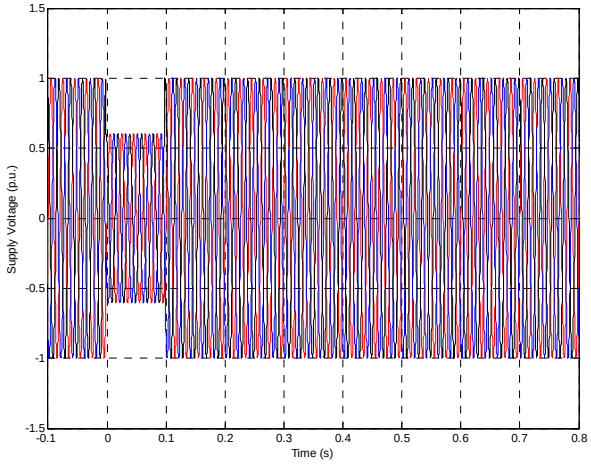

Stator line voltage (p.u.)

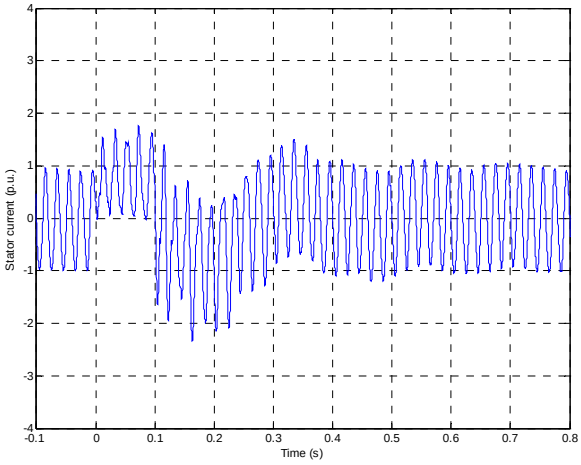

Phase B stator current (p.u.)

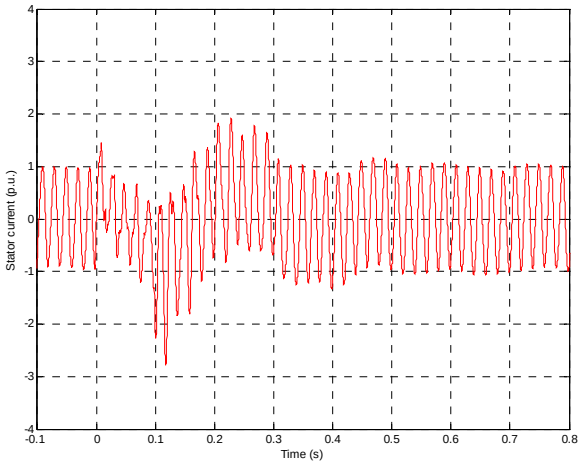

Phase A stator current (p.u.)

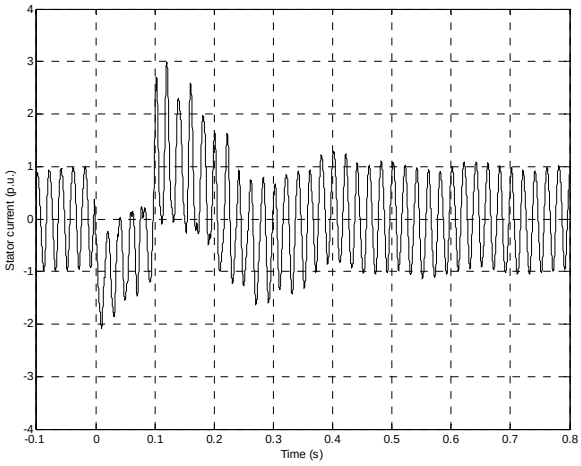

Phase C stator current (p.u.)

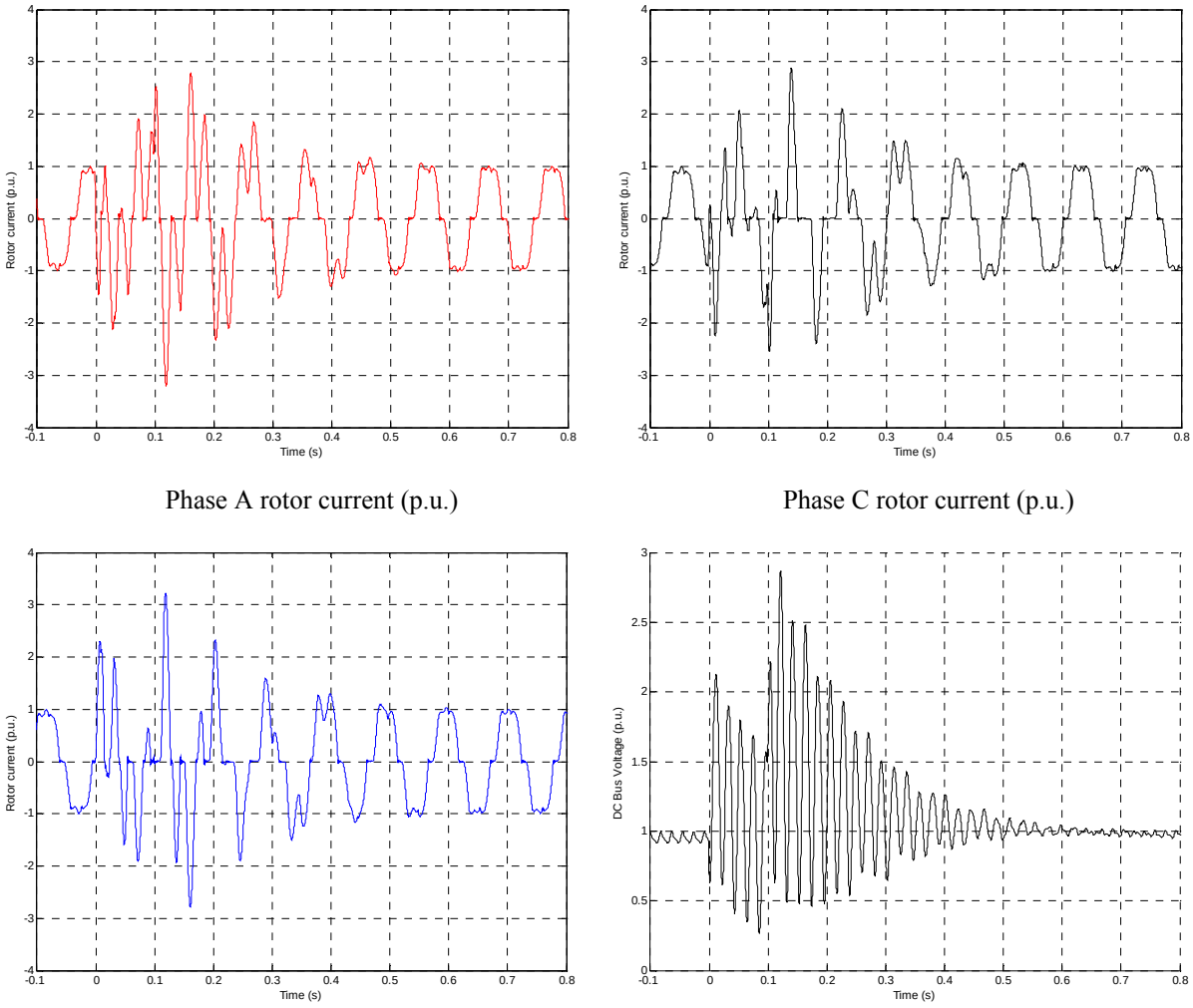

Figure A.3. 100 ms dip results (0.4 p.u. balanced three phase dip)

A.4.2 Single phase results

The following results are for a simulated 0.4. p.u. 100 ms single phase dip. This case is representative of all the single phase dip results. Better correlation with measured results was achieved for the single phase dips. Matching the exact instant of the voltage dip was essential for single phase dips as the response of the rotor circuit depends primarily on the flux linked by the stator winding that experiences the voltage dip.

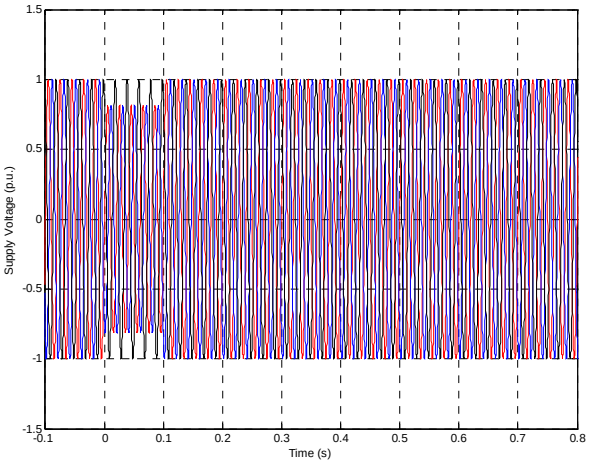

Stator line voltage (p.u.)

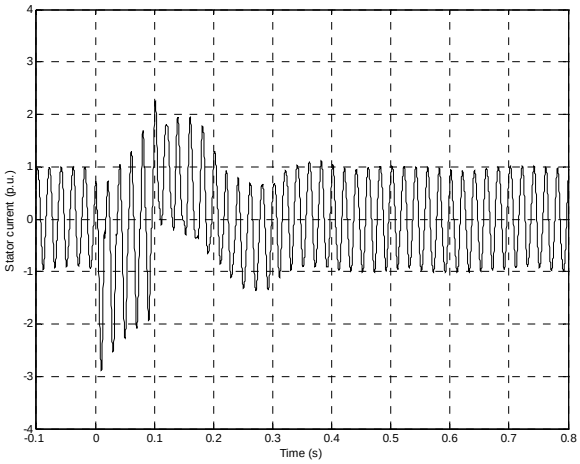

Phase C stator current (p.u.)

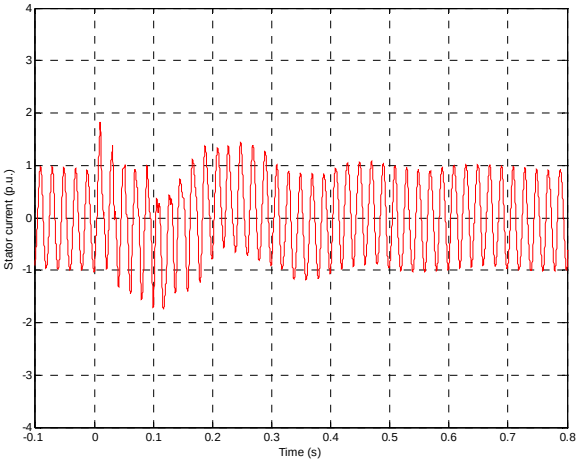

Phase A stator current (p.u.)

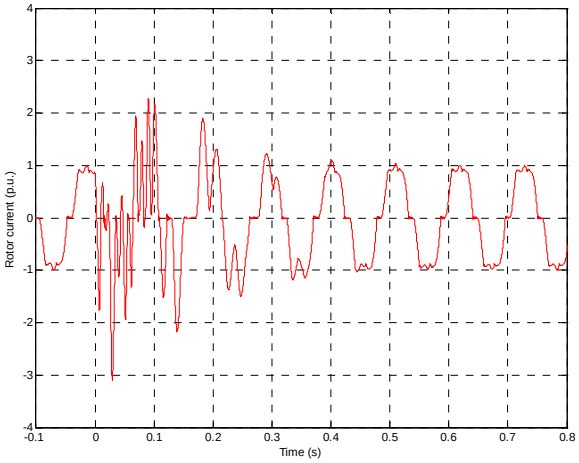

Phase A rotor current (p.u.)

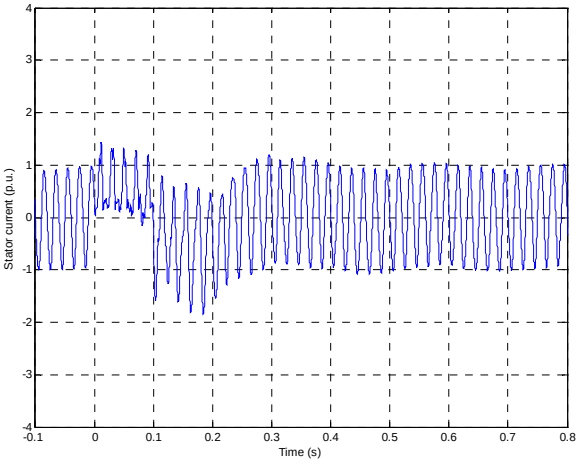

Phase B stator current (p.u.)

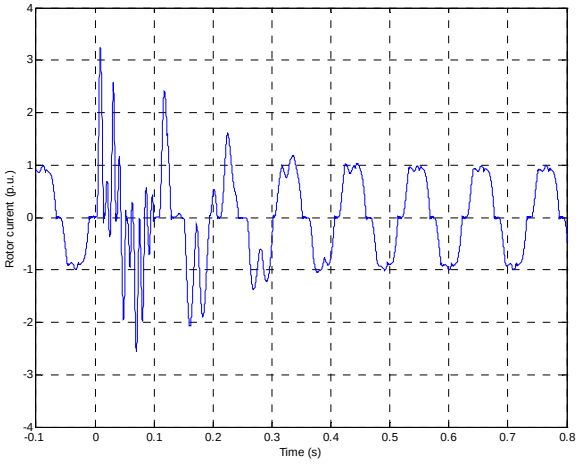

Phase B rotor current (p.u.)

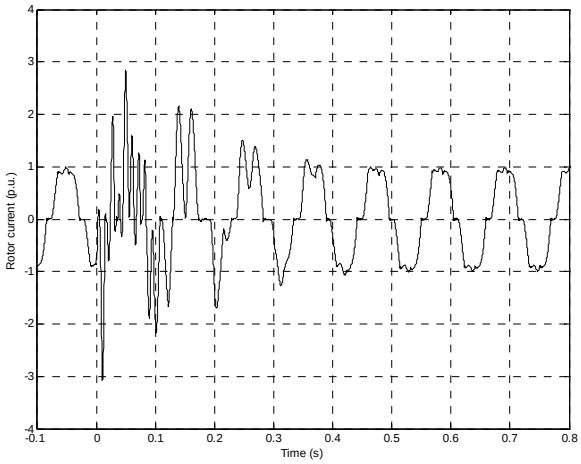

Phase C rotor current (p.u.)

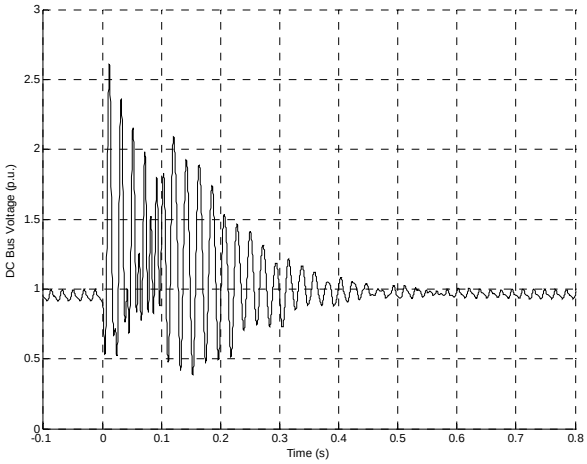

DC bus voltage (p.u.)

Figure A.4. 100 ms dip results (0.4 p.u. single phase dip)

Appendix B

Measurements

The following section presents a selection of the measured test results. Waveforms are presented for specific test cases showing the stator currents, rotor currents and DC bus voltage over the duration of the applied voltage dip. The test circuit and motor as presented in the paper was used for all measurements. The Eskom/Wits Voltage Dip Test Bed allows for accurate point on wave triggering of the voltage dip. This allows for repeatable test results for specific voltage dip parameters and loading conditions. The equipment used to record the measurements is shown in Table B.1.

Table B.1: Measurement equipment

Device	Model	Serial No
Oscilloscope	Tektronix TDS 544A 500 MHz	B011572
Voltage probe	Tektronix P5205 High Voltage Differential Probe	B020862
Current probes	Fluke 80i - 500s AC current probes	69018474 66919728 68815602
Tachometer	RS Digital photo tachometer RM-1501	385-0555

B.1 Three phase dips

For the balanced three phase dips the following parameters were kept constant:

A rotor resistance of 1.2 ohms connected across the DC bus was chosen such that at full load, the motor was operating at approximately 0.2 p.u. slip. A DC capacitance of 3.3 μF was chosen such that the full load steady state voltage ripple was limited to under 10 %. A constant load torque was applied to the motor for the duration of the test using a DC generator. By varying the field voltage of the DC generator, the induction motor was run at full load for the duration of each test.

B.1.1. 0.2 p.u balanced three phase dips

Voltage dips of magnitude 0.2 p.u. were applied for different dip durations. These tests were performed to analyse the transients generated by the rotor circuit of the motor in response to relatively minor voltage dips. Table B.2 shows a summary of the test results for 0.2 p.u. dips. The peak DC current and corresponding voltage transients as generated by the rotor circuit are shown. Figures B.1 – B.3 show a selection of the results.

Table B.2: Balanced three phase 0.2 p.u. dip results

Dip duration (ms)	Supply cycles	Maximum V_{dc}/I_{dc} (p.u.)
10	0.5	2.3
20	1.0	1.5
30	1.5	2.0
40	2.0	1.7
50	2.5	2.0
60	3.0	1.6
70	3.5	1.8
80	4.0	1.9
90	4.5	1.5
100	5.0	1.9
150	7.5	1.7
200	10.0	1.7
250	12.5	1.7

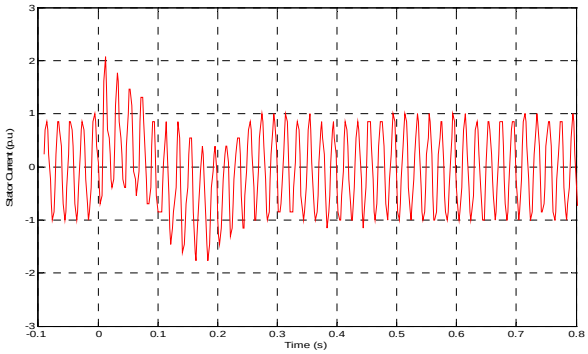

Phase A stator current (p.u.)

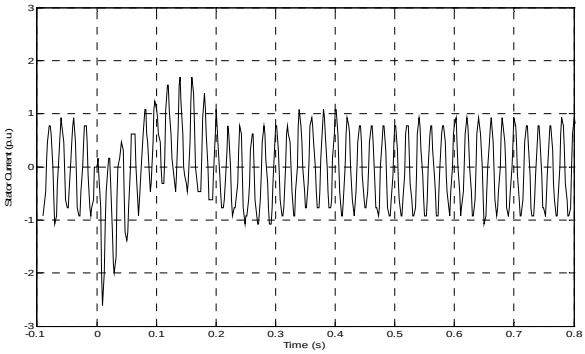

Phase B stator current (p.u.)

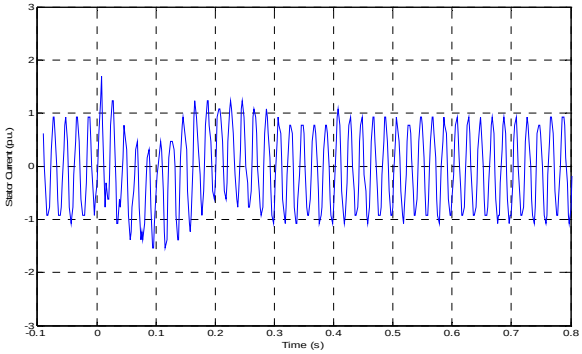

Phase C stator current (p.u.)

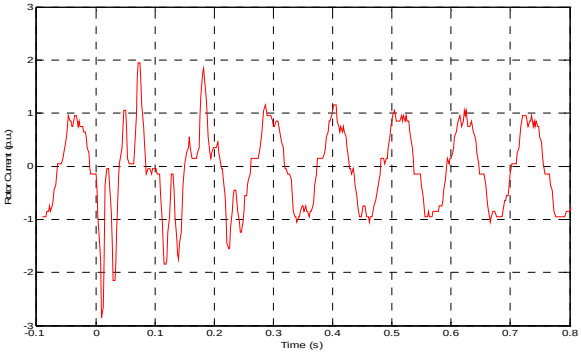

Phase A rotor current (p.u.)

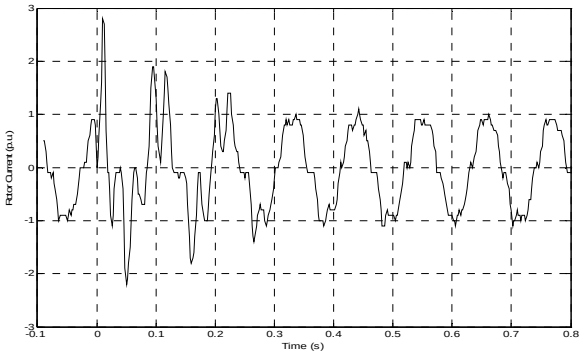

Phase B rotor current (p.u.)

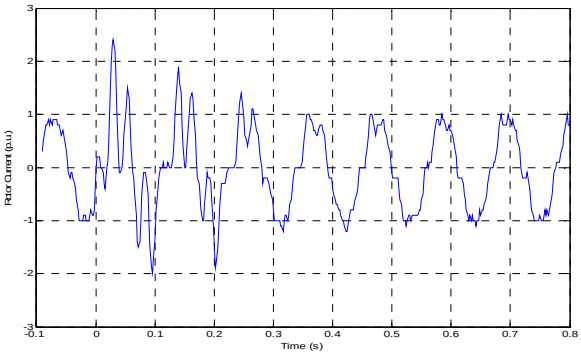

Phase C rotor current (p.u.)

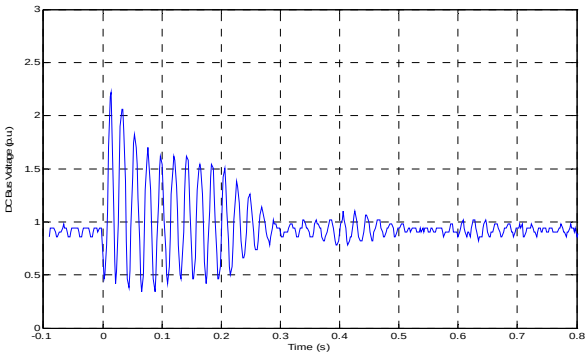

DC bus voltage (p.u.)

Figure B.1. 10 ms dip results (0.2 p.u. balanced three phase dip)

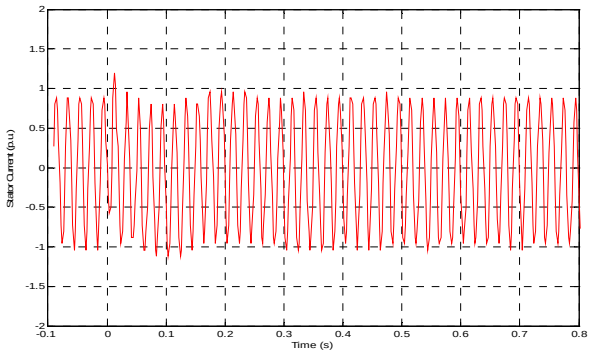

Phase A stator current (p.u.)

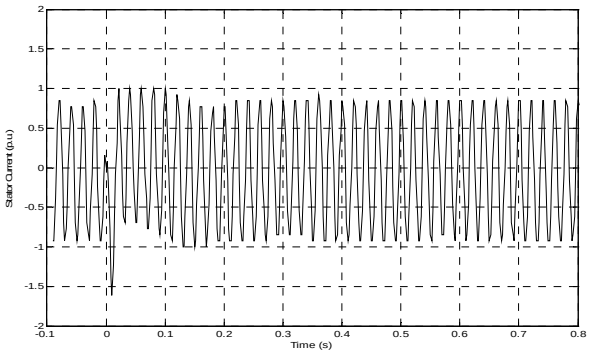

Phase B stator current (p.u.)

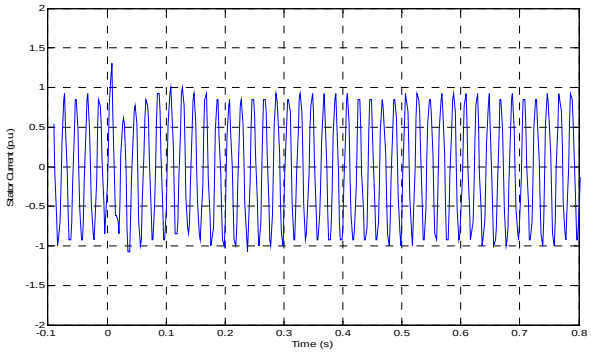

Phase C stator current (p.u.)

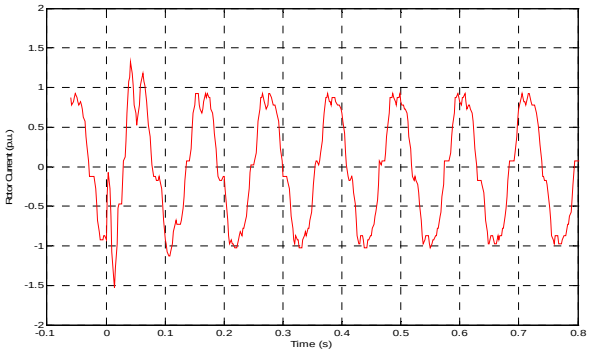

Phase A rotor current (p.u.)

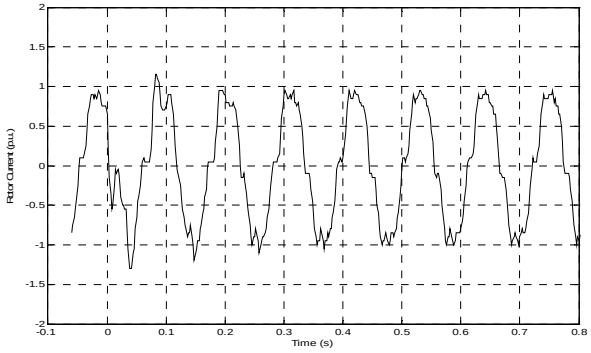

Phase B rotor current (p.u.)

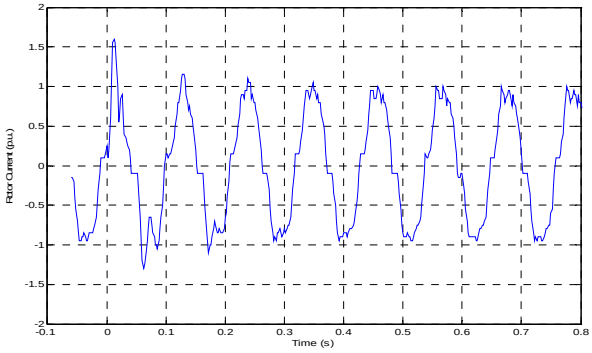

Phase C rotor current (p.u.)

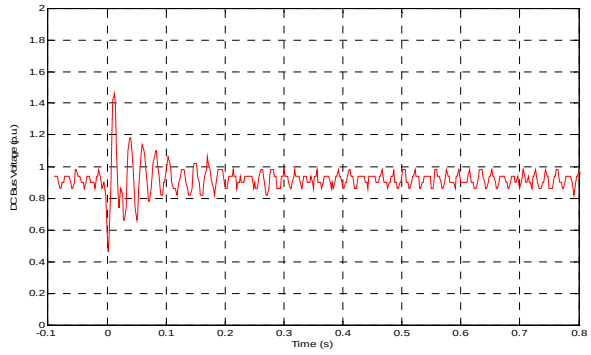

DC bus voltage (p.u.)

Figure B.2 20ms dip results (0.2 p.u. balanced three phase dip)

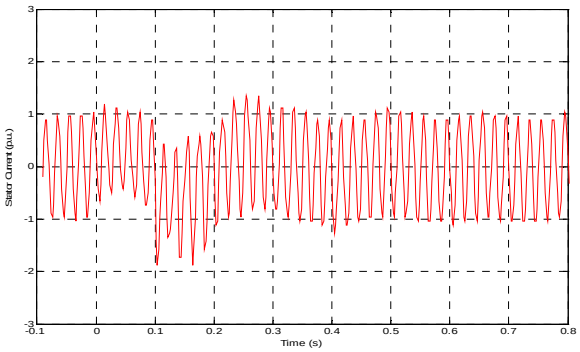

Phase A stator current (p.u.)

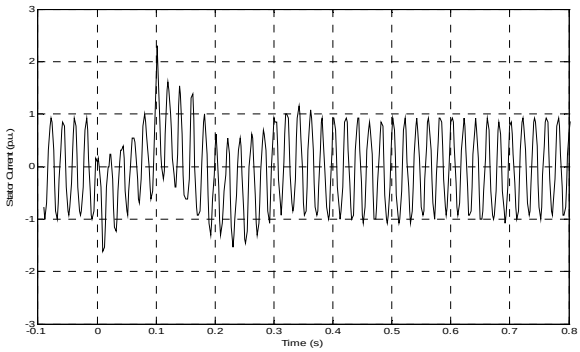

Phase B stator current (p.u.)

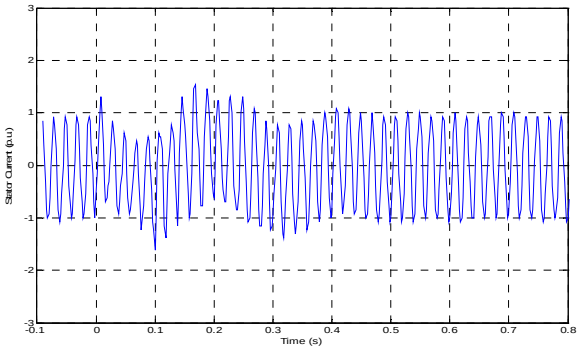

Phase C stator current (p.u.)

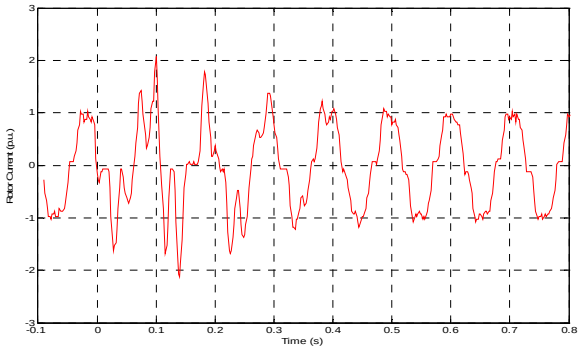

Phase A rotor current (p.u.)

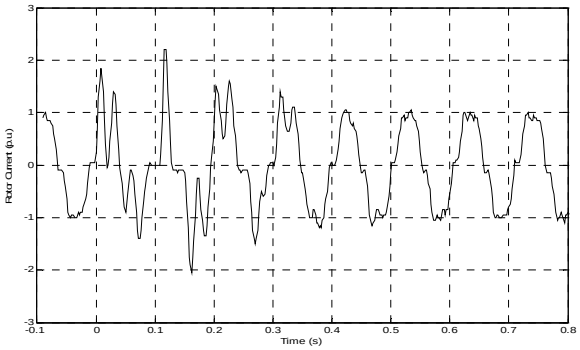

Phase B rotor current (p.u.)

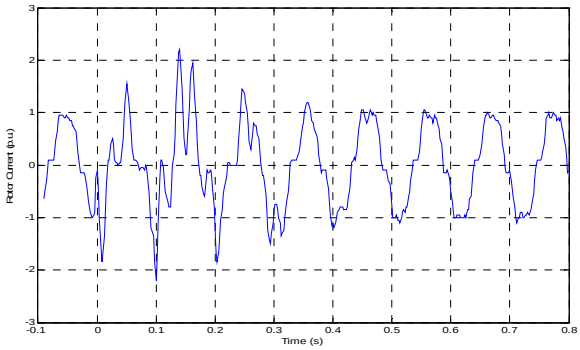

Phase C rotor current (p.u.)

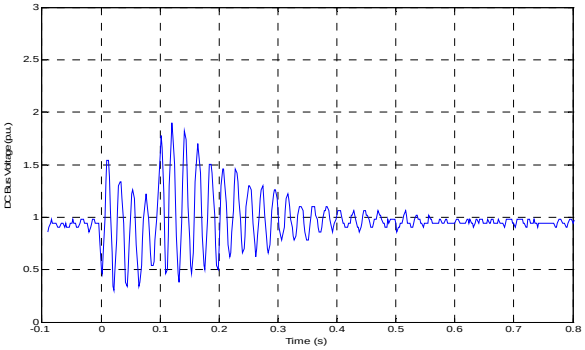

DC bus voltage (p.u.)

Figure B.3. 100 ms dip results (0.2 p.u. balanced three phase dip)

B.1.2. 0.4 p.u balanced three phase dips

Table B.3 shows a summary of the test results for 0.4 p.u. dips. The motor and SER circuit parameters were the same as specified for the 0.2 p.u. voltage dips.

Figures B.4 – B.6 show the measured waveforms for a 10 ms, 20 ms and 100 ms voltage dip. The similarities between these waveforms and the 0.2/0.6 p.u. dips are clearly visible. It is only the transient magnitudes that are different.

Table B.3: Balanced three phase 0.4 p.u. dip results

Dip duration (ms)	Supply cycles	Maximum V_{dc}/I_{dc} (p.u.)
10	0.5	3.3
20	1.0	1.9
30	1.5	3.1
40	2.0	2.0
50	2.5	2.9
60	3.0	2.2
70	3.5	2.7
80	4.0	2.6
90	4.5	2.3
100	5.0	2.7
150	7.5	2.0
200	10.0	2.7
250	12.5	2.0

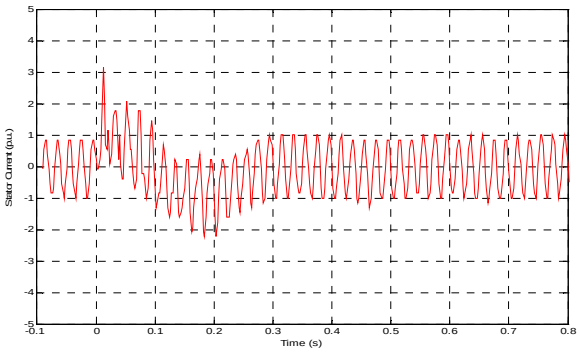

Phase A stator current (p.u.)

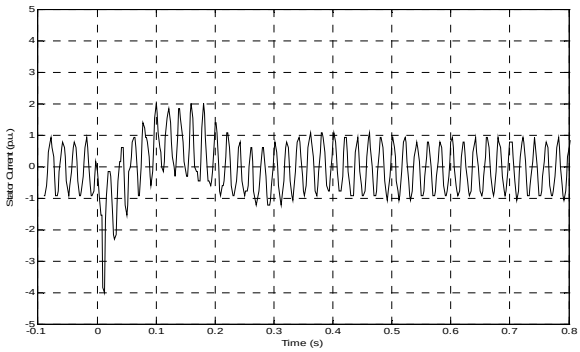

Phase B stator current (p.u.)

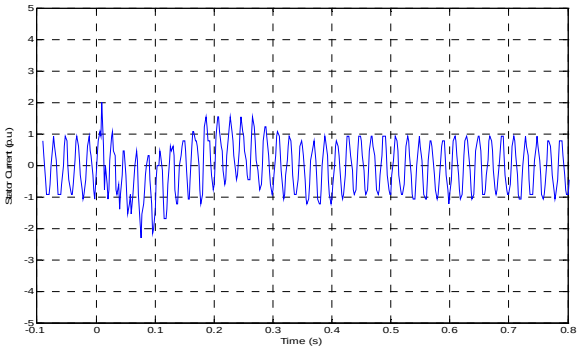

Phase C stator current (p.u.)

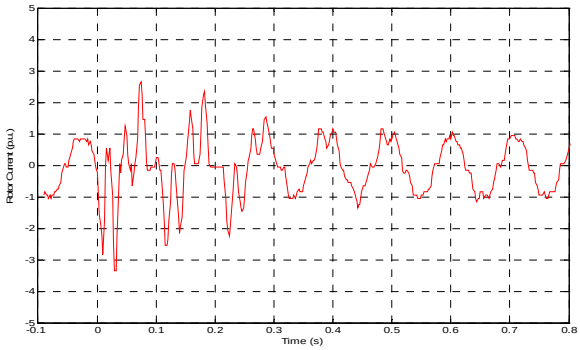

Phase A rotor current (p.u.)

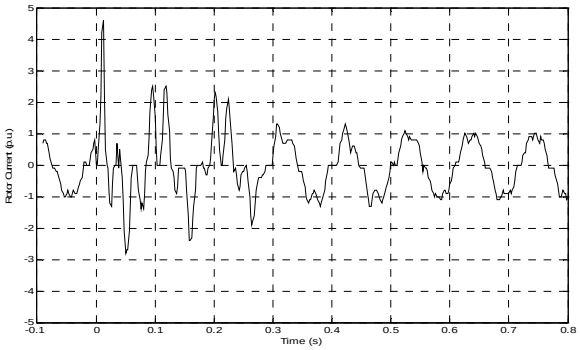

Phase B rotor current (p.u.)

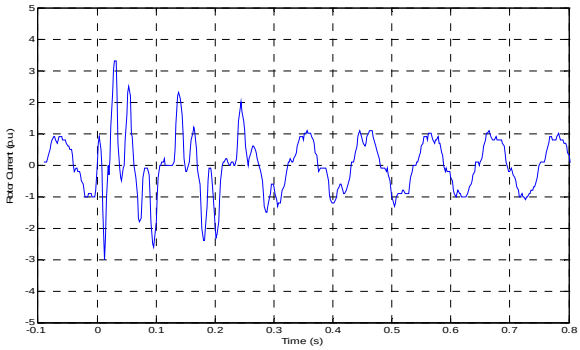

Phase C rotor current (p.u.)

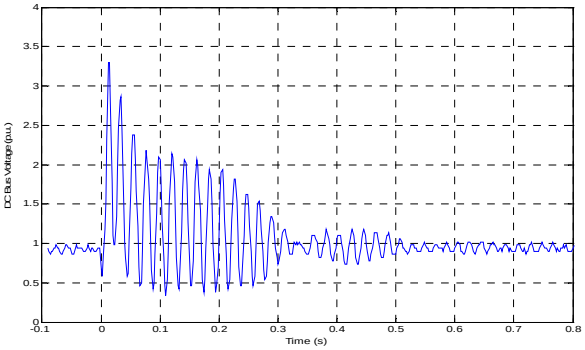

DC bus voltage (p.u.)

Figure B.4. 10 ms dip results (0.4 p.u. balanced three phase dip)

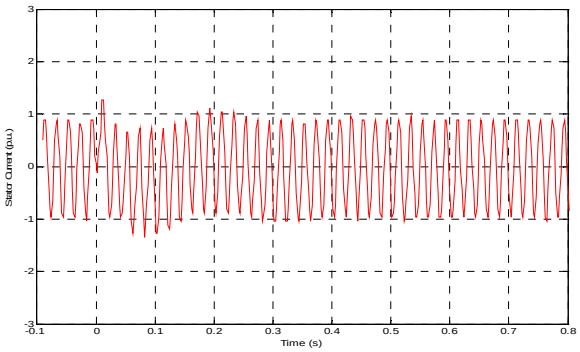

Phase A stator current (p.u.)

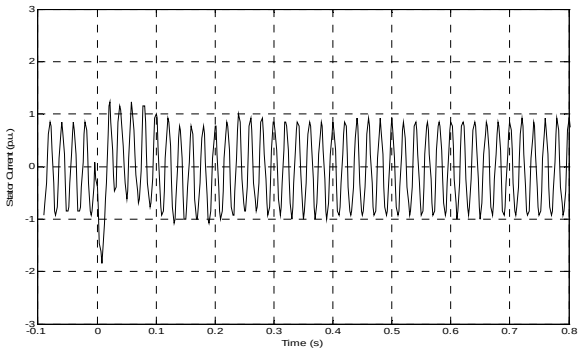

Phase B stator current (p.u.)

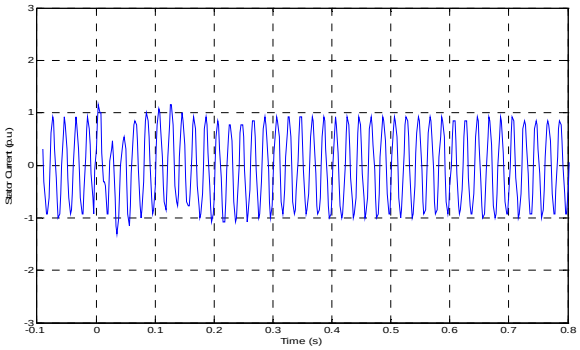

Phase C stator current (p.u.)

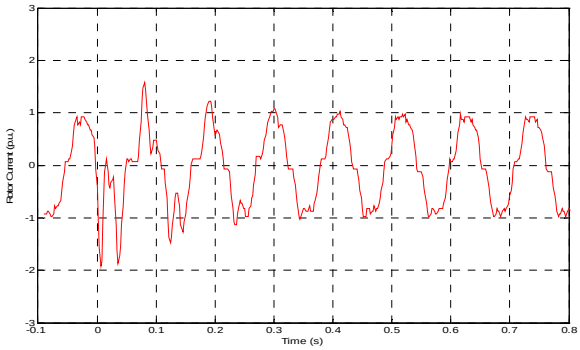

Phase A rotor current (p.u.)

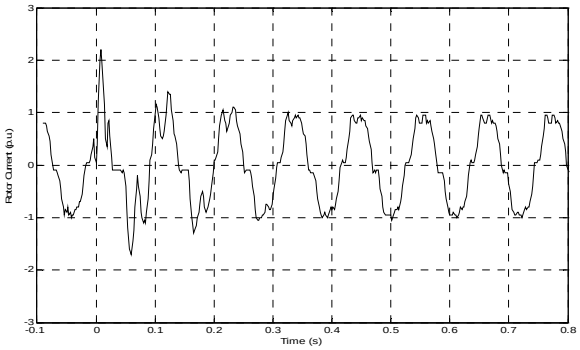

Phase B rotor current (p.u.)

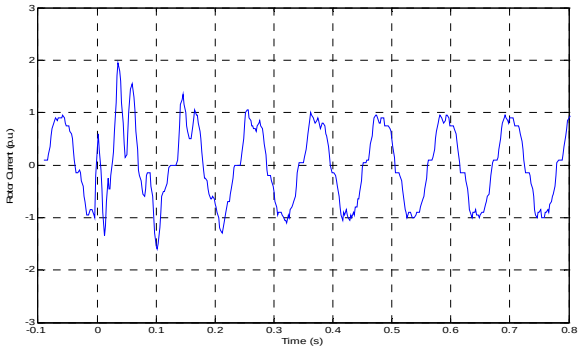

Phase C rotor current (p.u.)

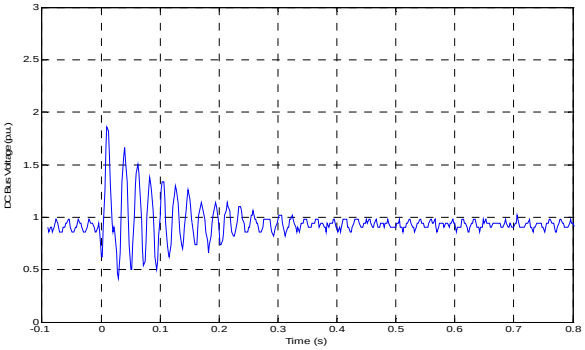

DC bus voltage (p.u.)

Figure B.5 20ms dip results (0.4 p.u. balanced three phase dip)

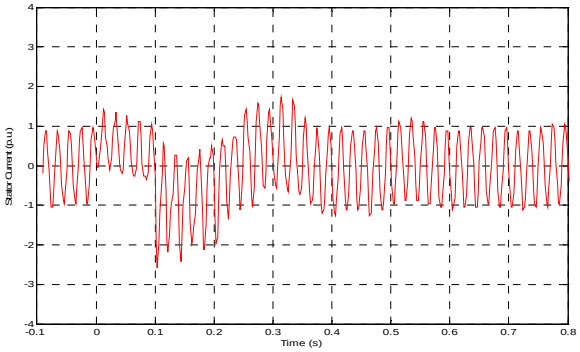

Phase A stator current (p.u.)

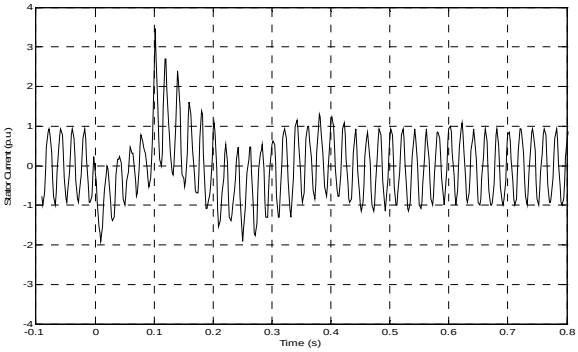

Phase B stator current (p.u.)

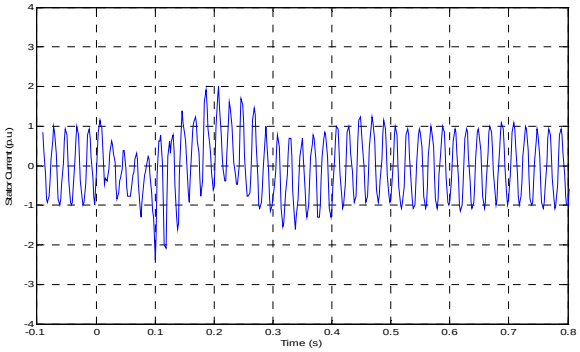

Phase C stator current (p.u.)

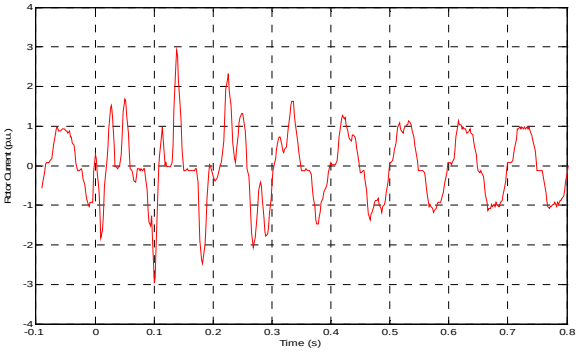

Phase A rotor current (p.u.)

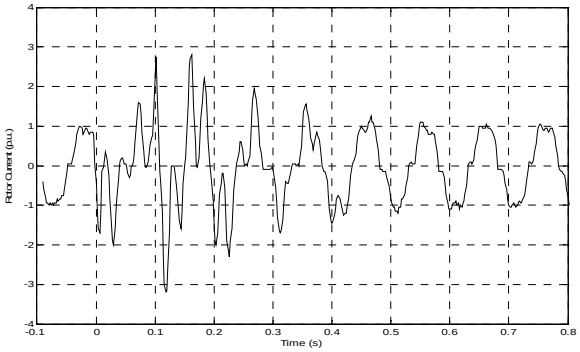

Phase B rotor current (p.u.)

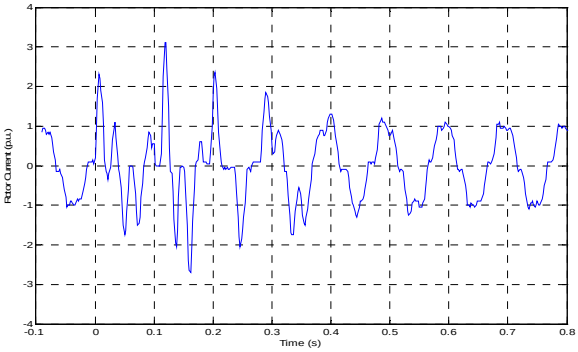

Phase C rotor current (p.u.)

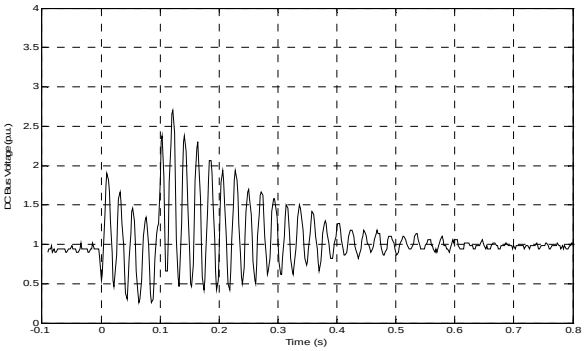

DC bus voltage (p.u.)

Figure B6. 100 ms dip results (0.4 p.u. balanced three phase dip)

B.1.3. 0.6 p.u balanced three phase dips

Table B.4 shows a summary of the test results for 0.6 p.u. dips. These particular test confirm that large magnitude dips cause severe rotor transients that may well exceed the ratings of the rotor side converters.

Figures B.7 – B.9 show a selection of waveforms for 0.6 p.u. dips.

Table B.4: Balanced three phase 0.6 p.u. dip results

Dip duration (ms)	Supply cycles	Maximum V_{dc}/I_{dc} (p.u.)
10	0.5	4.0
20	1.0	2.3
30	1.5	3.7
40	2.0	2.4
50	2.5	3.5
60	3.0	2.7
70	3.5	3.1
80	4.0	3.1
90	4.5	2.9
100	5.0	3.3
150	7.5	2.3
200	10.0	3.7
250	12.5	2.3

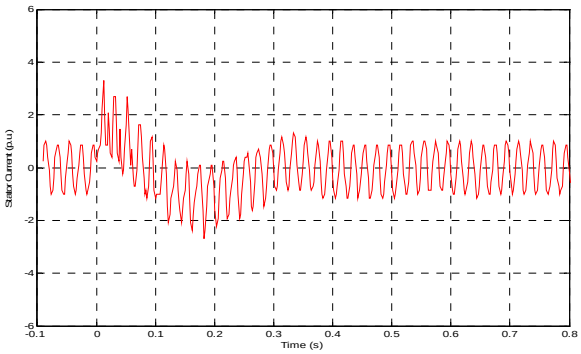

Phase A stator current (p.u.)

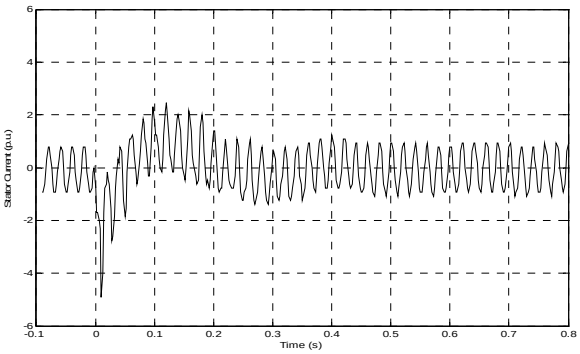

Phase B stator current (p.u.)

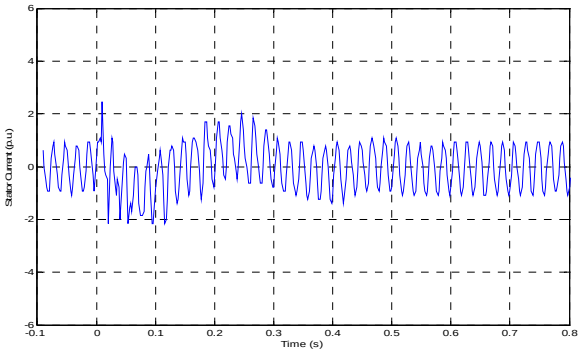

Phase C stator current (p.u.)

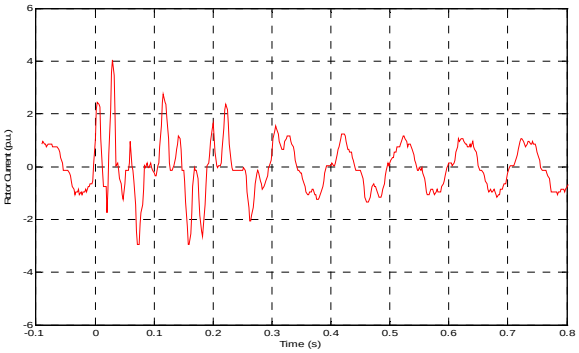

Phase A rotor current (p.u.)

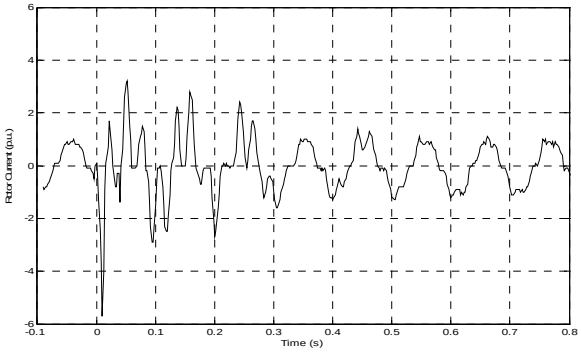

Phase B rotor current (p.u.)

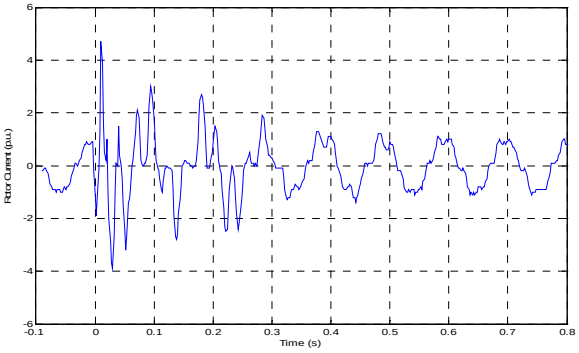

Phase C rotor current (p.u.)

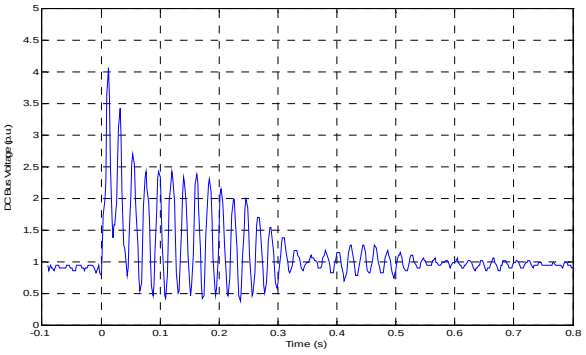

DC bus voltage (p.u.)

Figure B.7. 10 ms dip results (0.6 p.u. balanced three phase dip)

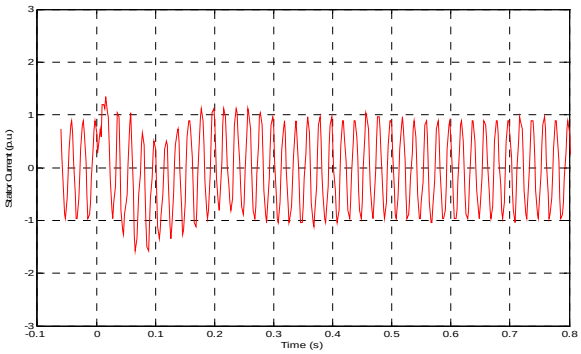

Phase A stator current (p.u.)

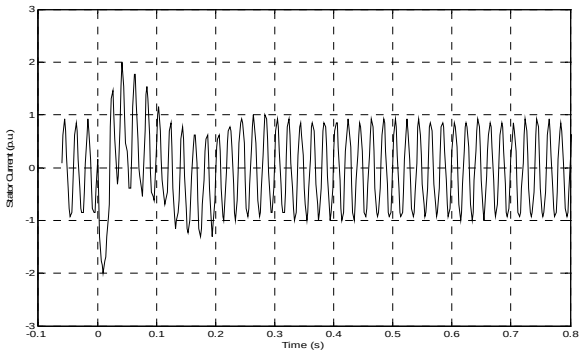

Phase B stator current (p.u.)

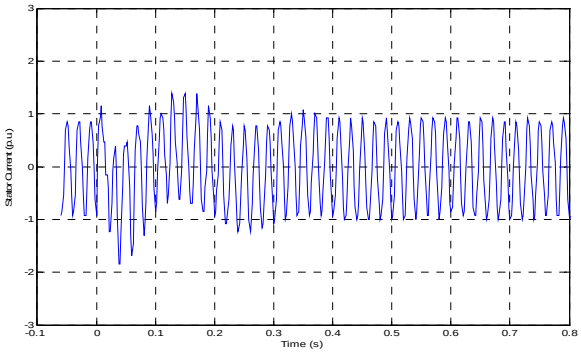

Phase C stator current (p.u.)

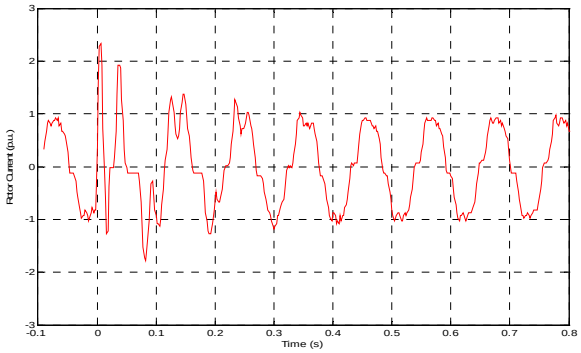

Phase A rotor current (p.u.)

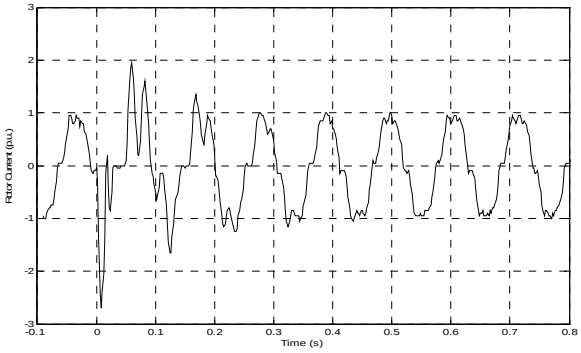

Phase B rotor current (p.u.)

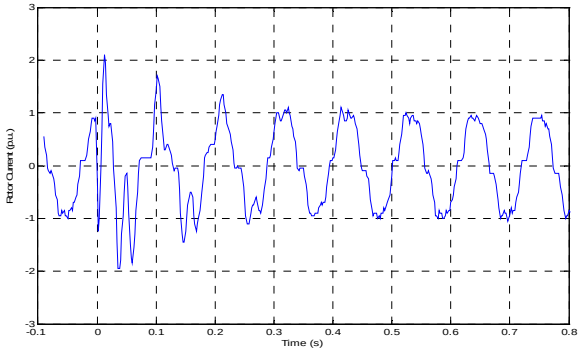

Phase C rotor current (p.u.)

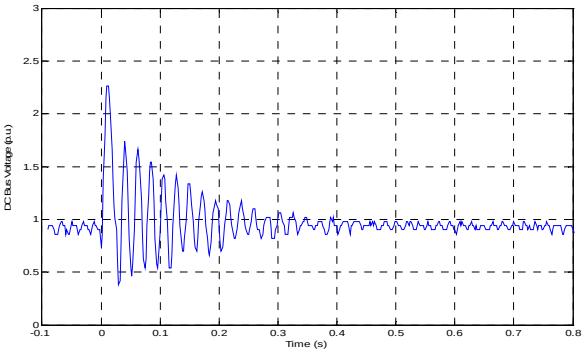

DC bus voltage (p.u.)

Figure B.8 20ms dip results (0.6 p.u. balanced three phase dip)

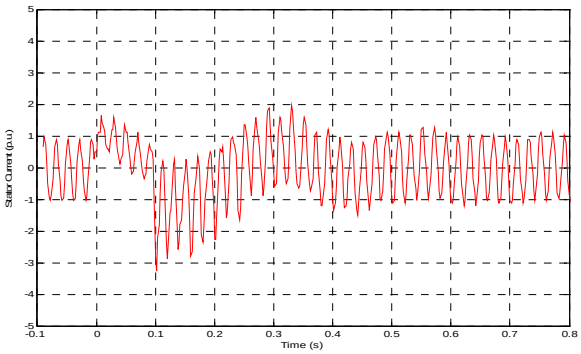

Phase A stator current (p.u.)

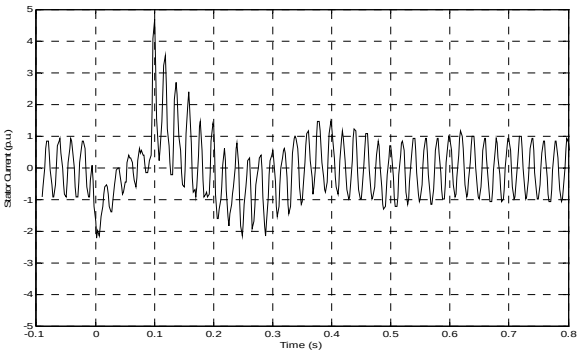

Phase B stator current (p.u.)

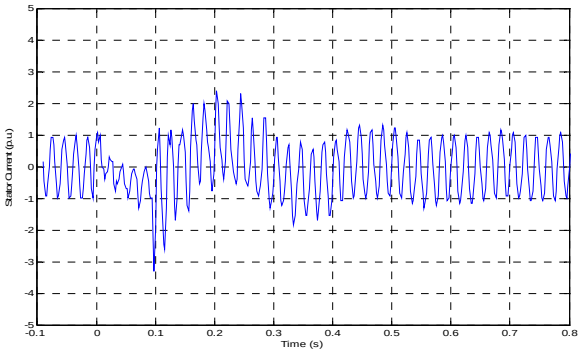

Phase C stator current (p.u.)

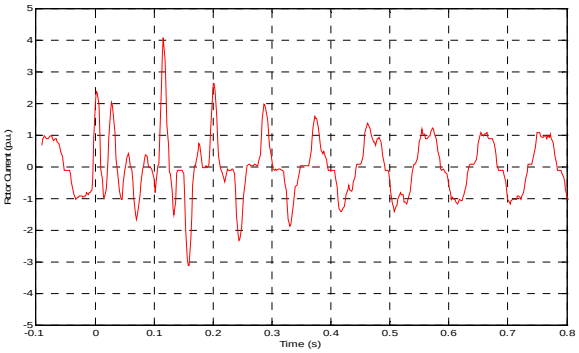

Phase A rotor current (p.u.)

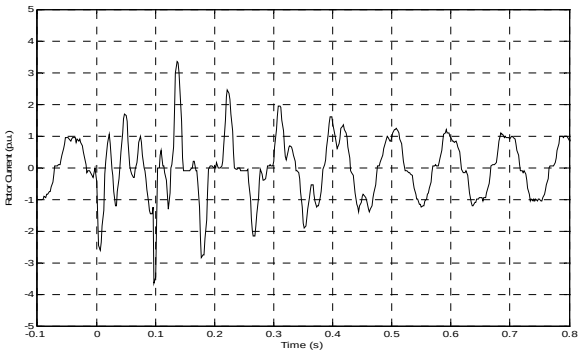

Phase B rotor current (p.u.)

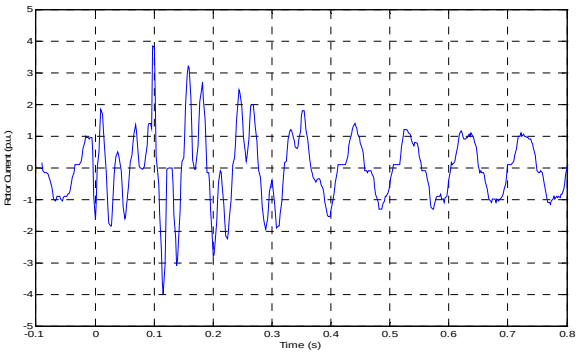

Phase C rotor current (p.u.)

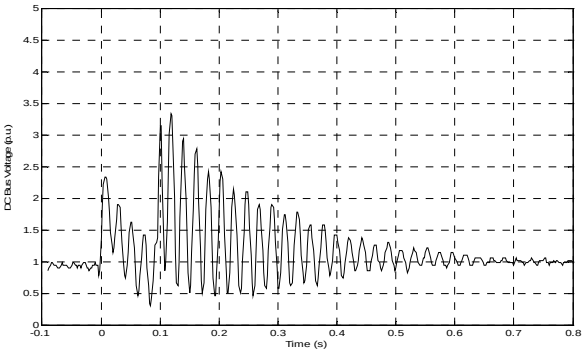

DC bus voltage (p.u.)

Figure B.9. 100 ms dip results (0.6 p.u. balanced three phase dip)

B.1.4. Discussion of balanced three phase dip results

The following results are clear from the three phase measurements:

1. The maximum rotor current and voltage for balanced three phase dips occur at the instant of voltage recovery.

2. The voltage dip magnitude and duration are the most significant parameters that determine the maximum rotor transients.

3. Voltage dips with duration of whole cycles cause minimum transients and dips with duration of half cycles cause maximum current and torque transients.

4. Shorter dips produce significantly larger transients than longer dips. Flux held stationary with respect to the stator windings introduces substantial phase differences between the applied voltage and induced emf in the motor windings. The severity of this phenomenon is dependant on the time constant of the DC component of flux.

5. Although three phase dips are less common than single phase dips, they tend to be more severe. A severe three phase dip will cause problems to rotor circuit converters as transients of well over 2 p.u. have been measured.

B.2 Single phase dips

The following section presents the results of the single phase voltage dip tests. The motor and SER circuit parameters are the same as for the three phase dips. The motor was run at full load with a rotor resistance of 1.2 ohms such that the speed of the motor was 0.2 p.u. slip.

The current transients generated as a result of a single phase dip depend primarily on the flux linking that particular phase winding at the instant of the dip. For single phase dips the voltage dip duration is not as significant as for three phase dips. The maximum transients are produced at the instant of the voltage dip and not at the point of recovery. The magnitude of the voltage dip and the instantaneous flux linkage of the phase winding that experiences the dip are the significant parameters and determine the response of the rotor circuit. Table B.5 shows a selection of single phase dip results to illustrate the recorded results. Figures B.10 and B.11 show the effect of the stator flux linkage for a single phase 10 ms dip.

Table B.5: Single phase dip results

Dip magnitude (p.u.)	Dip duration (ms)	Flux linkage of winding	Maximum V_{dc}/I_{dc} (p.u.)
0.2	10	Min	1.2
0.2	10	Max	1.9
0.4	10	Min	1.5
0.4	10	Max	2.8
0.6	10	Min	1.8
0.6	10	Max	3.5
0.4	50	Max	2.5
0.4	100	Max	2.5
0.4	250	Max	2.6

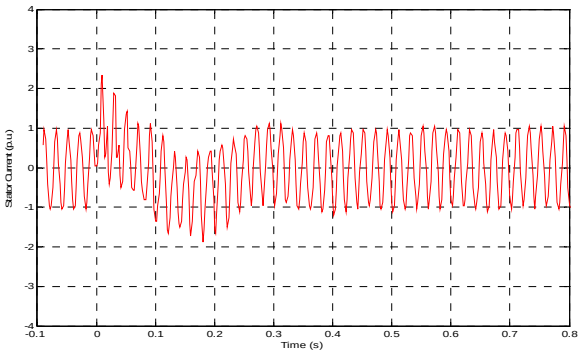

Phase A stator current (p.u.)

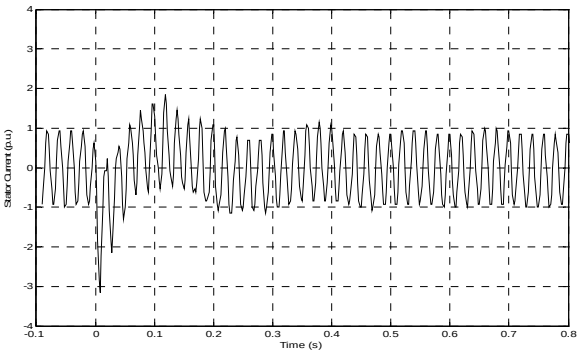

Phase B stator current (p.u.)

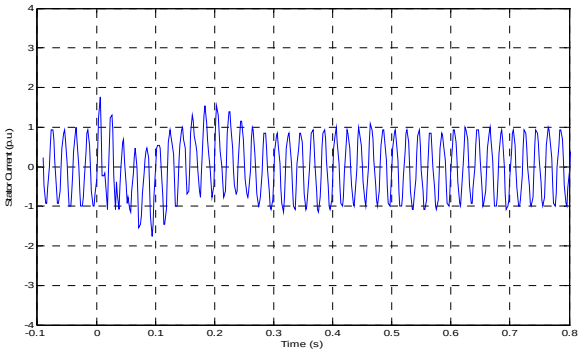

Phase C stator current (p.u.)

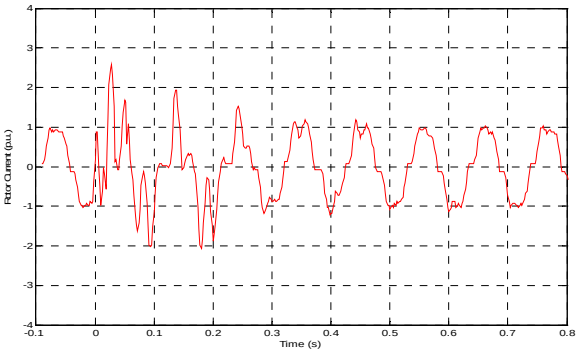

Phase A rotor current (p.u.)

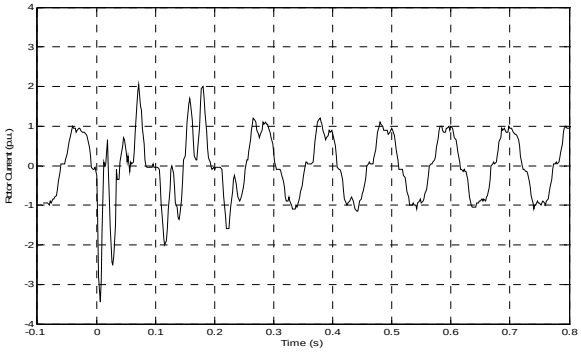

Phase B rotor current (p.u.)

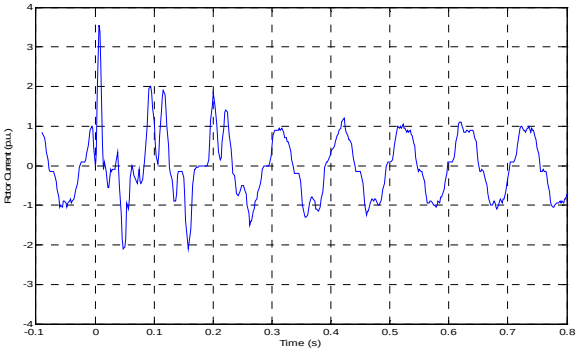

Phase C rotor current (p.u.)

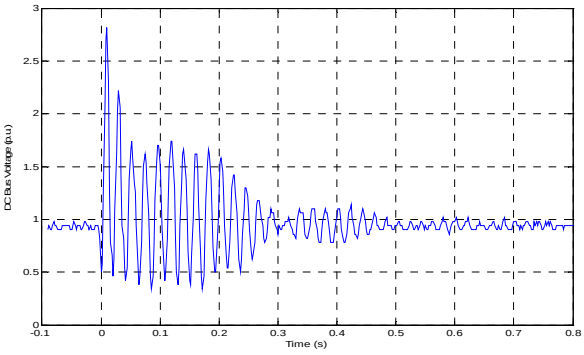

DC bus voltage (p.u.)

Figure B.10. 10 ms dip results (0.4 p.u. single phase dip – maximum flux linkage)

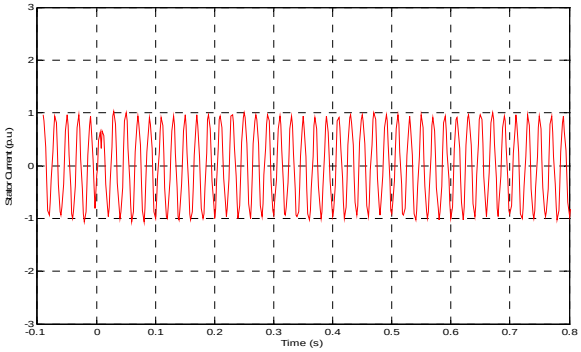

Phase A stator current (p.u.)

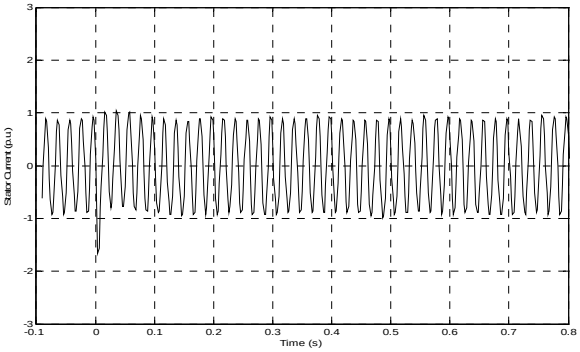

Phase B stator current (p.u.)

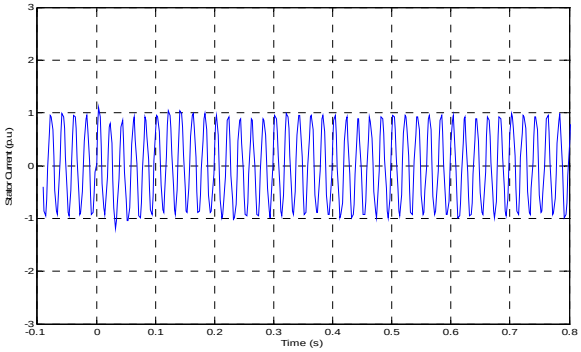

Phase C stator current (p.u.)

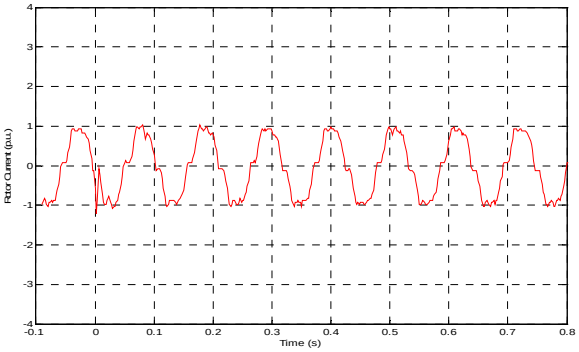

Phase A rotor current (p.u.)

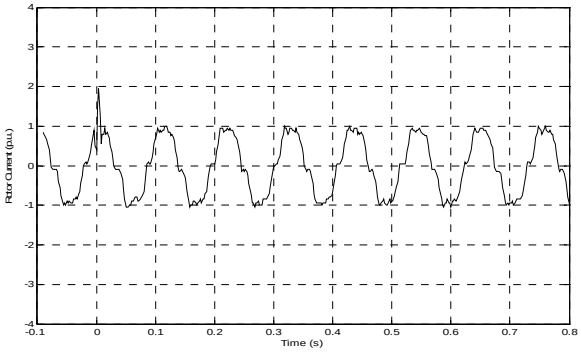

Phase B rotor current (p.u.)

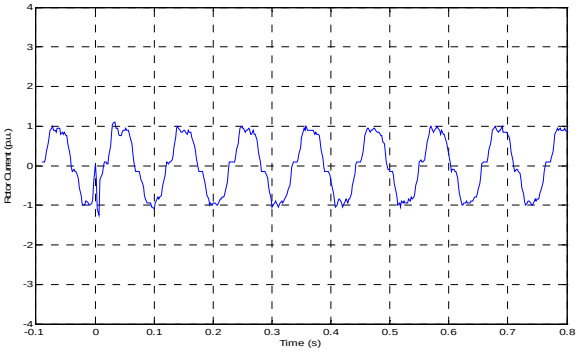

Phase C rotor current (p.u.)

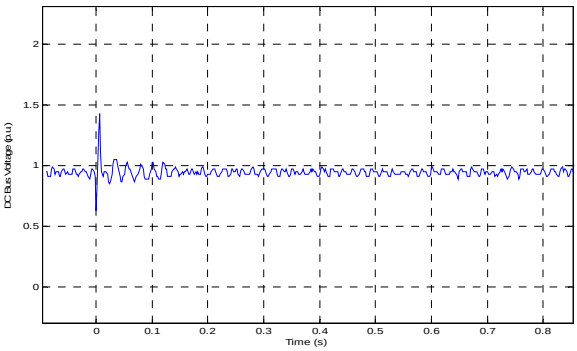

DC bus voltage (p.u.)

Figure B.11. 10 ms dip results (0.4 p.u. single phase dip – minimum flux linkage)

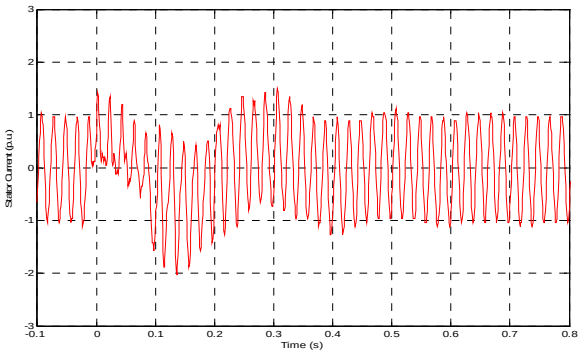

Phase A stator current (p.u.)

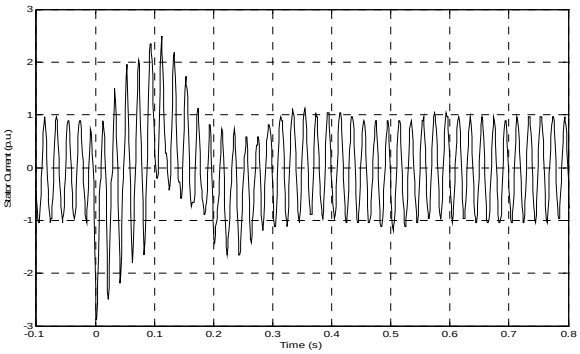

Phase B stator current (p.u.)

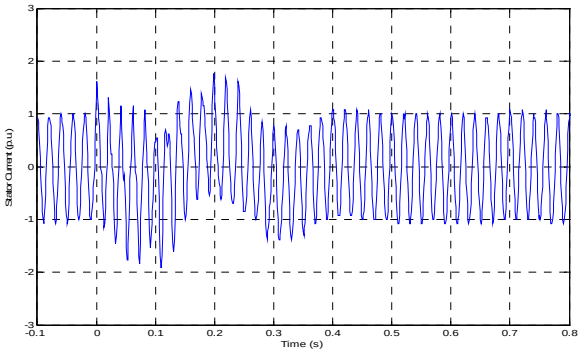

Phase C stator current (p.u.)

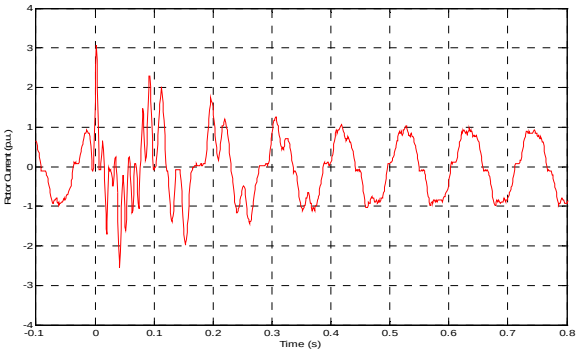

Phase A rotor current (p.u.)

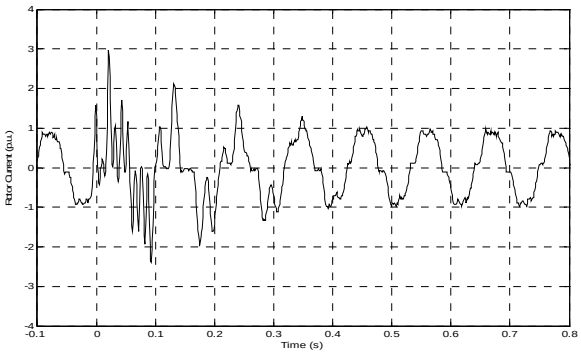

Phase B rotor current (p.u.)

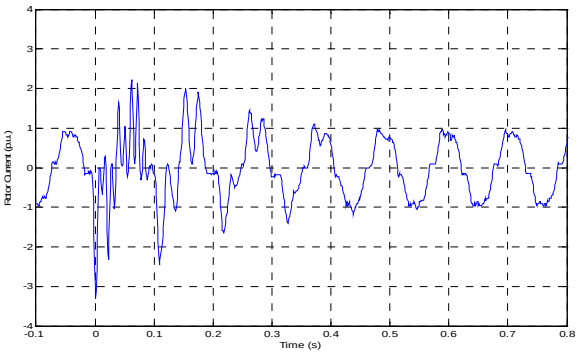

Phase C rotor current (p.u.)

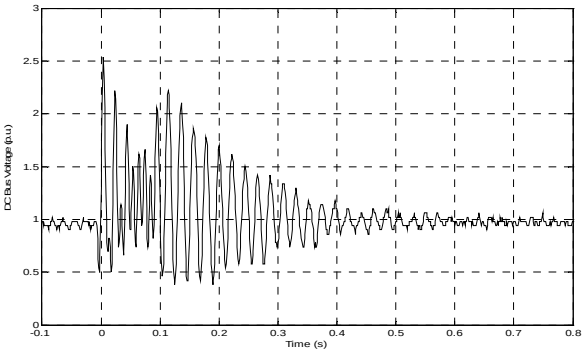

DC bus voltage (p.u.)

Figure B.12. 100 ms dip results (0.4 p.u. single phase dip – maximum flux linkage)

B.2.1. Discussion of single phase dip results

The following results are clear from the single phase measurements:

1. The maximum rotor transients are produced at the instant of the voltage dip and not at the point of voltage recovery.

2. The current transients generated as a result of a single phase dip depend primarily on the flux linking that particular phase winding at the instant of the dip. Thus, the point on the 50 Hz cycle at which the voltage dip occurs is most significant for the generation of rotor transients.

3. For single phase dips the voltage dip duration is not as significant as for three phase dips.

4. The magnitude of the voltage dip and the instantaneous flux linkage of the phase winding that experiences the dip are the significant parameters and determine the response of the rotor circuit.

B.3 Varied rotor resistance

Tests were performed to see how operation at different slip speeds altered the response of the rotor circuit to a dip. The rotor resistances synthesised by the converters determine the dynamic response of the motor to a voltage disturbance. This resistance governs the speed for a particular load condition. The greater the rotor resistance the more damped the transient currents injected into the DC bus appear to be. This is most obvious for the three phase dip case at voltage recovery.

In this case, the rotor resistance was set at 0.4 ohms which corresponded to a motor speed of 0.1 p.u. slip at full load. The effects of various balanced three phase voltage dips were tested on the SER circuit. The dynamic response of the motor depends primarily on the size of the synthesised rotor resistance (in this case the resistance across the DC bus). The smaller the resistance, the greater the rotor currents injected into the DC bus. Table B.6 shows a summary of the test results.

Table B.6: 0.4 ohm rotor resistance three phase dip results

Dip magnitude (p.u.)	Dip duration (ms)	Maximum V_{dc}/I_{dc} (p.u.)
0.2	10	2.8
0.4	10	4.5
0.6	10	5.0
0.2	50	1.7
0.4	50	3.0
0.6	50	4.3
0.2	100	2.0
0.4	100	3.4
0.6	100	4.5

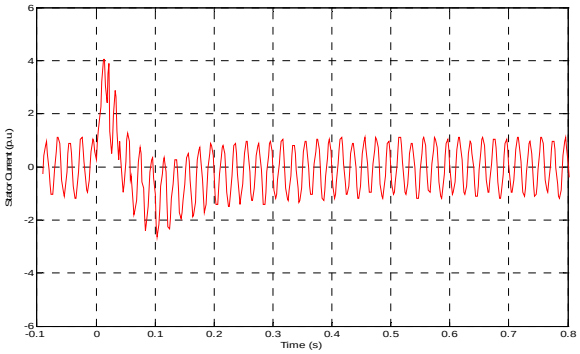

Phase A stator current (p.u.)

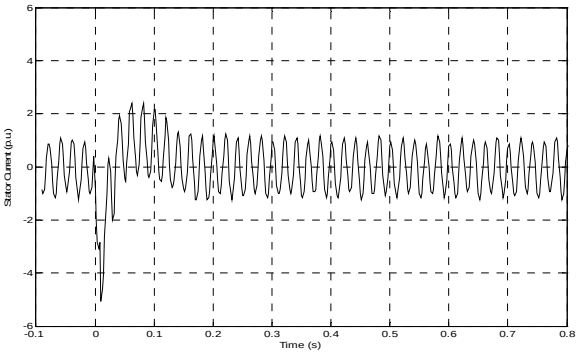

Phase B stator current (p.u.)

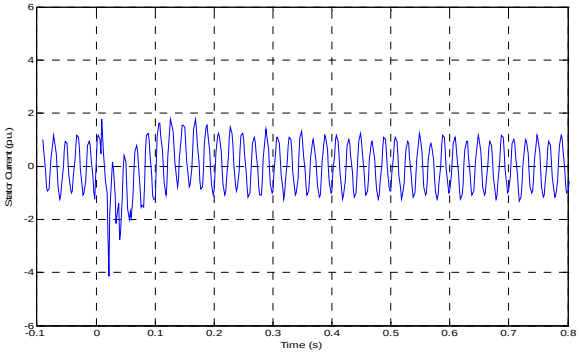

Phase C stator current (p.u.)

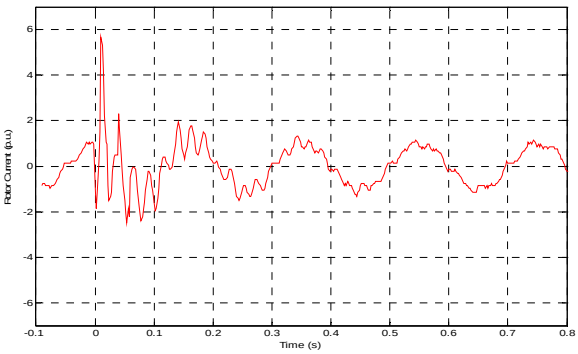

Phase A rotor current (p.u.)

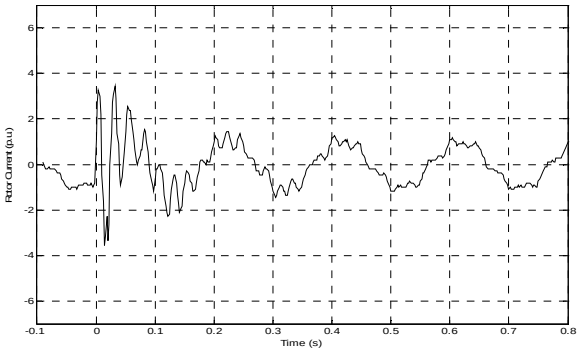

Phase B rotor current (p.u.)

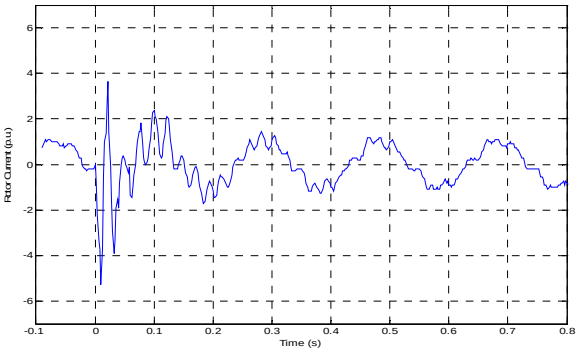

Phase C rotor current (p.u.)

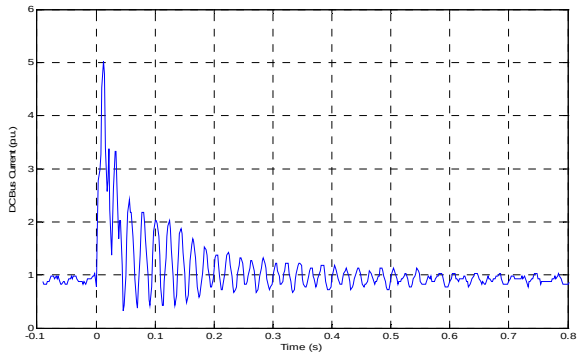

DC bus voltage (p.u.)

Figure B.13. 10 ms dip results (0.6 p.u. three phase dip – 0.4 ohm rotor resistance)

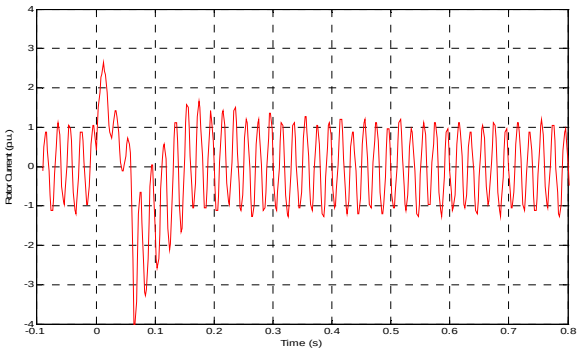

Phase A stator current (p.u.)

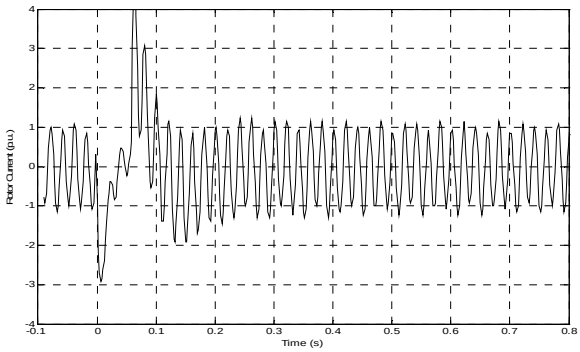

Phase B stator current (p.u.)

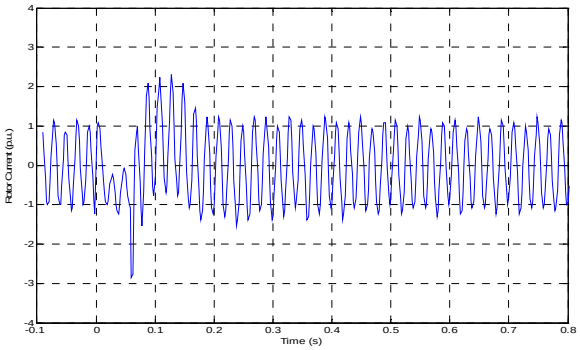

Phase C stator current (p.u.)

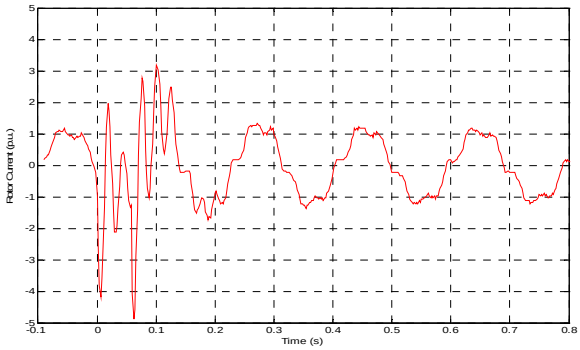

Phase A rotor current (p.u.)

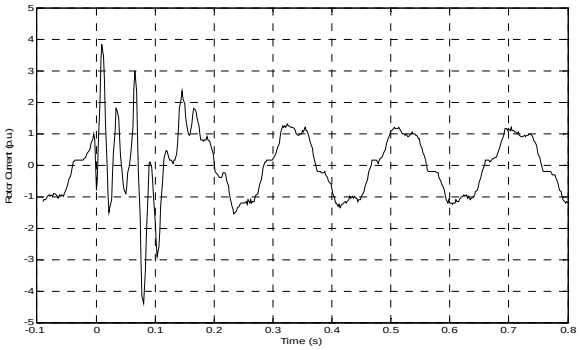

Phase B rotor current (p.u.)

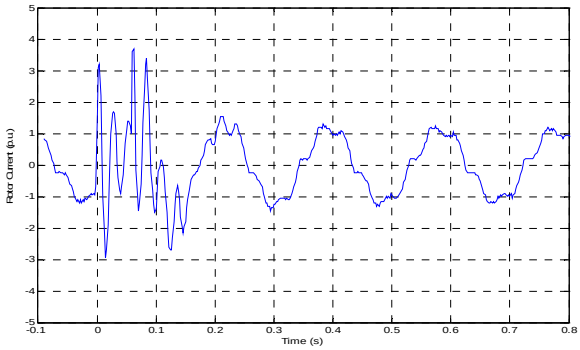

Phase C rotor current (p.u.)

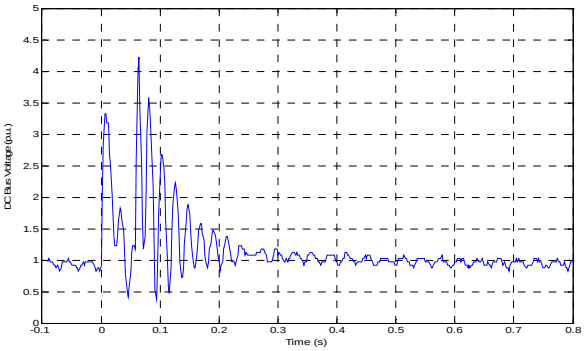

DC bus voltage (p.u.)

Figure B.14. 50 ms dip results (0.6 p.u. three phase dip – 0.4 ohm rotor resistance)

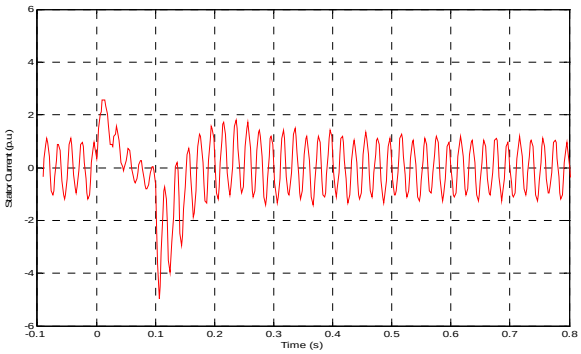

Phase A stator current (p.u.)

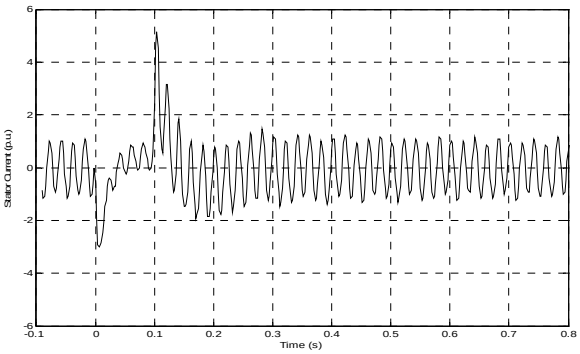

Phase B stator current (p.u.)

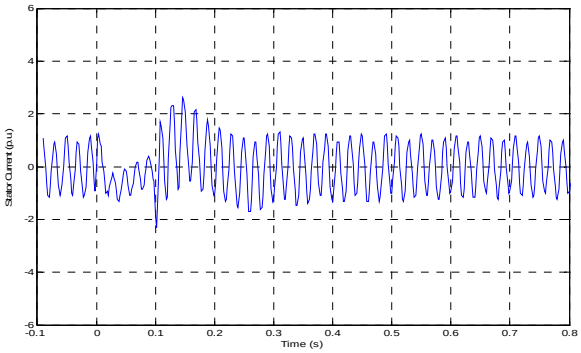

Phase C stator current (p.u.)

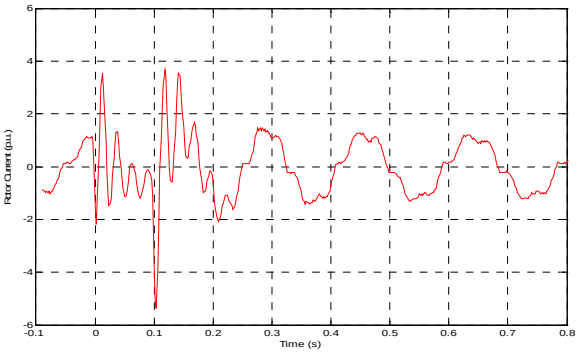

Phase A rotor current (p.u.)

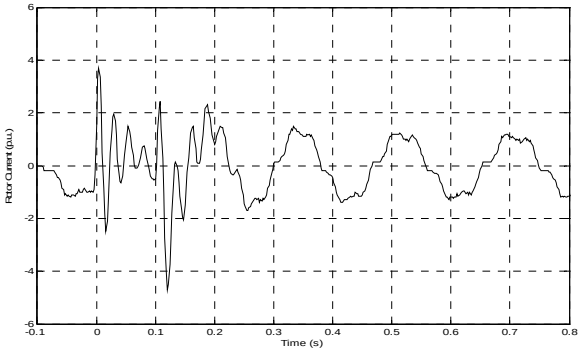

Phase B rotor current (p.u.)

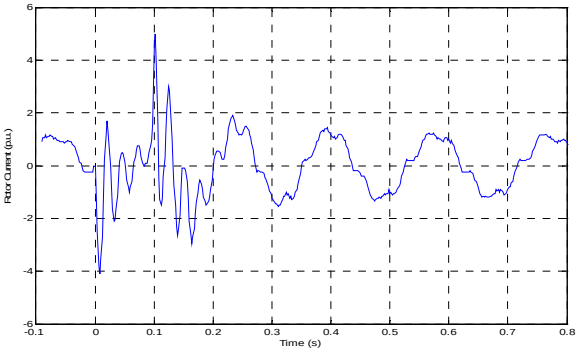

Phase C rotor current (p.u.)

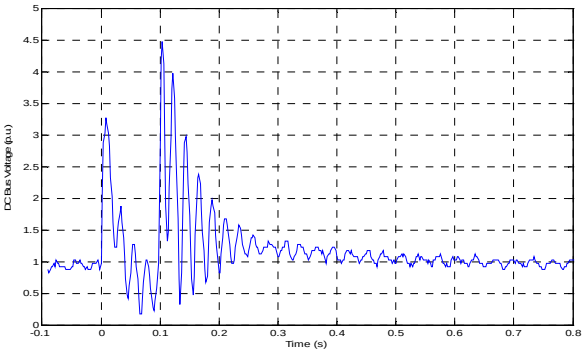

DC bus voltage (p.u.)

Figure B.15. 100 ms dip results (0.6 p.u. three phase dip – 0.4 ohm rotor resistance)

References

[1] H. K. Lauw, W. S. Meyer, Universal machine modelling for the representation of rotating electrical machinery in an electromagnetic transients program, *IEEE Transactions on Power Apparatus and Systems*, v PAS-101, n 6, Jun 1982, pp 1342-1351.

[2] Leuven EMTP Centre, Alternative Transients Program Rule Book, Leuven, Belgium, 1992.

[3] P. K. Kovacs, Transient Phenomena in Electrical machines, Elsevier, New York, 1984.

[4] J. M. Van Coller, Variable Speed AC Machine Drives, ELEN 599 course notes, University of the Witwatersrand. 2004.

[5] D.W. Novotny, T. A. Lipo, Vector Control and Dynamics of AC Drives, Oxford University Press, 1997.

[6] M. G. Say, The Performance and Design of Alternating Current Machines, Sir Isaac Pitman & Sons LTD, 3rd edition, 1968.